

THE EFFECT OF SOFT IRONCORE LAMINATION REMOVAL TOWARDS
COGGING TORQUE IN AN ELECTRIC GENERATOR



AKHTAR RAZUL RAZALI

For the fulfillment of

Final Report

for The

FRGS RDU160134

UMP

Automotive Engineering Center (AEC)

Faculty of Mechanical Engineering

UNIVERSITI MALAYSIA PAHANG

31ST JULY 2018

ACKNOWLEDGEMENT

The researchers would like to address their gratitude to the Kementerian Pendidikan Tinggi Malaysia (KPT) and Universiti Malaysia Pahang for the financial assistance through RDU 160134. Special thanks also go to Mr. Yap Wee Leong and Mr. Syaiful Azlan A Rahman, who is very dedicated to keep this project running and successfully graduated their Master Degree. Not to forget, to those helpful teaching engineers, Mr. Aziha, Mr. Asmizam, Mr. Rozikin and Mr. Hafietz for their trust (for the machineries usage), support and helpful advice whenever they were needed. Special thanks to Mr. Nazrul Idzham for the FE simulation analysis assistance throughout the project, Miss Hasinah Shariff for her assistance of analysis and administration/report writing/preparation. Many thanks too to those who contributed towards this project directly and indirectly.

Finally, to the team, special and warm thanks for the commitment shown to drive this project to success. Without everyone's contribution, this project will never see this happy ending.



UMP

ABSTRAK

The generator that normally used in the market, which is the iron-cored electricity generator has high cogging and starting torques. By redesigning of the iron-cored electricity generator, Axial-flux Permanent Magnet (AFPM) configuration minimizes the usage of ferrite material. AFPM, one of the coreless electricity generator configuration has a less counter electromotive force (CEMF) compare to the cored electricity generator. AFPM configuration also has no cogging torque and low starting torque. Application of a coreless electricity generator is the most suitable compare to the cored electricity generator. However, it is expected that the elimination of the ferrite material within the coreless electricity generator itself increases the power generation. The configuration is the ironless electricity generator. This thesis presents the analysis of the AFPM ironless electricity generator. There are two main testing present in this thesis, open circuit test and close circuit test. The result of the analysis shows that the rotational speed proportionally with voltage output for open circuit test. The close circuit test shown power proportionally with rotational speed.

The logo of the University of Muhammadiyah Palembang (UMPP) is a large, downward-pointing arrow. The arrow is divided into four quadrants by a vertical and a horizontal line. The top-left and bottom-right quadrants are light blue, while the top-right and bottom-left quadrants are light purple. The letters 'UMPP' are written in white, bold, sans-serif font across the center of the arrow.

UMPP

ABSTRACT

Penjana elektrik yang biasanya digunakan dalam pasaran, yang merupakan penjana elektrik yang menggunakan teras besi mempunyai *cogging* dan daya kilas permulaan yang tinggi. Dengan mereka bentuk semula penjana elektrik yang menggunakan teras besi, konfigurasi Axial-fluks Magnet kekal (AFPM) mengurangkan penggunaan bahan logam. AFPM, salah satu konfigurasi penjana elektrik tanpa teras yang mempunyai *counter electromotive force* (CEMF) yang kurang berbanding dengan penjana elektrik menggunakan teras besi. Konfigurasi AFPM juga tidak mempunyai *cogging torque* dan daya kilas permulaan yang rendah. Penggunaan penjana elektrik tanpa teras adalah yang paling sesuai berbanding dengan penjana elektrik dengan teras. Walau bagaimanapun, ia dijangka bahawa penghapusan bahan logam dalam penjana elektrik tanpa teras sendiri akan meningkatkan penjana kuasa. Konfigurasi adalah penjana elektrik tanpa teras. Tesis ini akan membentangkan analisis penjana elektrik tanpa teras AFPM. Terdapat dua ujian utama di dalam tesis ini, ujian secara litar terbuka dan ujian secara litar tertutup. Hasil analisis menunjukkan bahawa kelajuan putaran berkadaran dengan voltan keluaran untuk ujian litar terbuka. Kuasa yang dihasilkan berkadaran dengan kelajuan putaran bagi ujian litar tertutup.



UMP

TABLE OF CONTENT

DECLARATION	
TITLE PAGE	
ACKNOWLEDGEMENTS	ii
ABSTRAK	iii
ABSTRACT	iv
TABLE OF CONTENT	v
LIST OF TABLES	viii
LIST OF FIGURES	ix
LIST OF SYMBOLS	xi
LIST OF ABBREVIATIONS	xii
CHAPTER 1 INTRODUCTION	1
1.1 Research Background	1
1.2 Research Objectives	2
1.3 Research Scope	3
CHAPTER 2 LITERATURE REVIEW	4
2.1 Electricity Generation	4
2.1.1 Magnetic Field	5
2.1.2 Concept Regarding Magnetic Field Cutting	7
2.2 Ironcore Electricity Generator	9
2.2.1 Element and Working Principle	9
2.2.2 Attraction between Ironcore Lamination and Permanent Magnets	11

2.2.3	Cogging Torque in An Ironcore Generator	11
2.3	Ironless Coreless Generator	12
2.3.1	Axial Flux Permanent Magnet	13
2.3.2	Structure of Axial Flux Permanent Magnet	14
2.3.3	Types of magnet in Ironless Coreless Generator	16
2.3.4	Coil Design for the Ironless Coreless Generator	17
2.3.5	Gap Distance between Magnets	19
2.3.6	Number of Poles and Coils for the Ironless Coreless Generator	21
2.4	Electrical Waveform	22
2.4.1	Waveform Characteristic	22
2.4.2	Periodic Waveforms	23
2.4.3	Ripple on Electrical Waveform	25
CHAPTER 3 METHODOLOGY		27
3.1	Introduction	27
3.2	Fabrication Rotor and Stator for the Ironless Coreless Electricity Generator	29
3.3	Assembly Magnet to Rotor	32
3.4	Assembly Ironless Coreless Generator	33
3.5	Open Circuit Test on Ironless Coreless Electricity Generator	35
3.6	Closed Circuit Test on Ironless Coreless Electricity Generator	39
CHAPTER 4 RESULTS AND DISCUSSION		42
4.1	Fabrication and Assembly Issue	42
4.1.1	Part Warping	42
4.1.2	Collision	43
4.1.3	Assembly coil on stator	44

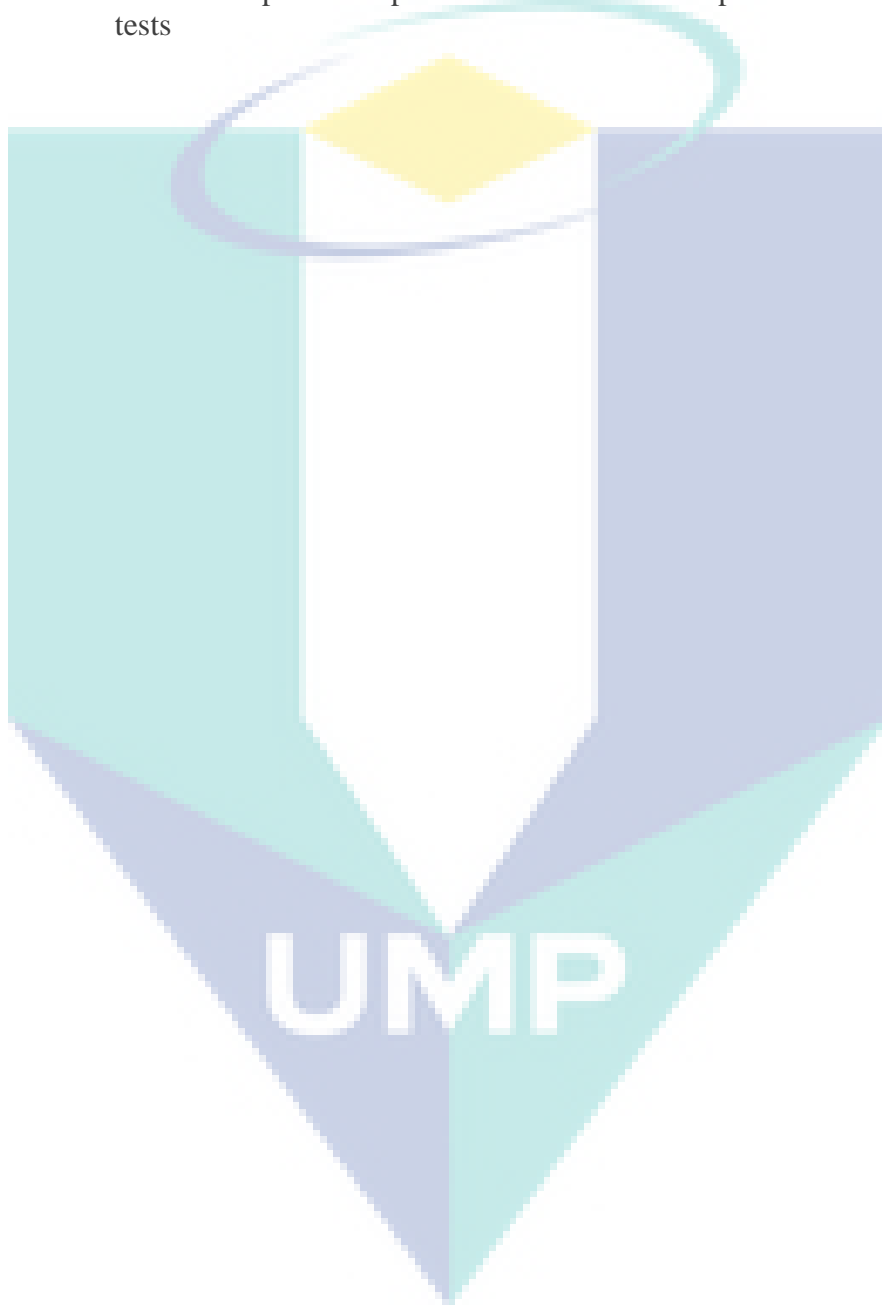
4.1.4	Rubbing and Wobbling	44
4.2	RESULTS AND DISCUSSION OF OPEN CIRCUIT TEST	47
4.2.1	Verification No Of Pole	51
4.2.2	Different Amplitude Each Phase Voltage	53
4.2.3	The Waveform Not Sinusoidal At Certain Speed	56
4.3	RESULTS AND DISCUSSION OF CLOSED CIRCUIT TEST	57
CHAPTER 5 CONCLUSION AND SUGGESTION		63
5.1	Conclusion	63
5.2	Suggestions	64
REFERENCES		65
APPENDIX A SAMPLE APPENDIX 1		65
APPENDIX B SAMPLE APPENDIX 2		70



UMP

LIST OF TABLES

Table 4.1	Result output voltage and wave frequency with various rotational speed	49
Table 4.2	The data of different amplitude each phase	55
Table 4.3	Results for power output in various rotational speed constant load tests	59



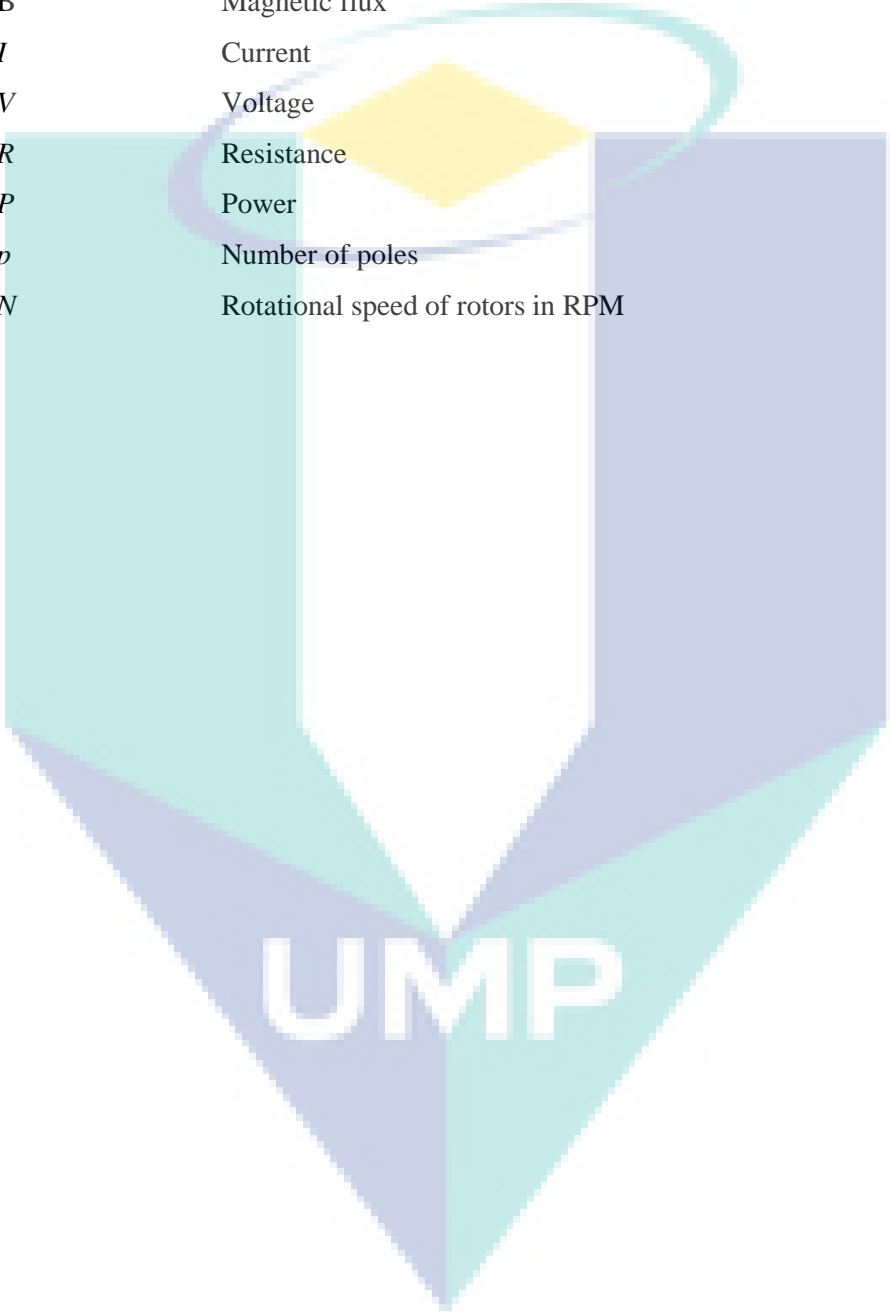
LIST OF FIGURES

Figure 2.1	Electricity Transportation	5
Figure 2.2	Figure shows the differences in line density in weaker and stronger magnetic fields	6
Figure 2.3	Magnetic field lines due to an infinite wire carrying current I .	6
Figure 2.4	Fleming's left-hand rule on magnetic field	7
Figure 2.5	Fleming's right-hand rule on magnetic field	8
Figure 2.6	Illustration shows the various position of armature as well as generator terminal voltage in various position of armature	10
Figure 2.7	Differences between Radial Flux Permanent Magnet Generator and Axial Flux Permanent Magnet Generator	14
Figure 2.8	The arrangement magnets on the rotor (N-S type)	15
Figure 2.9	Example of coil winding of one phase in a 12-pole pair AFPM machine with single –layer trapezoidal windings.	16
Figure 2.10	Coil dimension for the axial-flux permanent magnet generator	18
Figure 2.11	Approximated power of the generator via the different relative thickness of coil (c/τ)	19
Figure 2.12	Approximated power of the generator varies on air-gap distance	20
Figure 2.13	A sine wave waveform	24
Figure 3.1	Flow chart for Ironless Coreless Generator	28
Figure 3.2	Process flow for machining process	30
Figure 3.3	Fabrication using CNC Milling Machine	31
Figure 3.4	Fabrication Stator	31
Figure 3.5	Fabrication Rotor	32
Figure 3.6	Magnet assembled into rotor	33
Figure 3.7	Sequence process for assemble prototype ironless coreless generator	34
Figure 3.8	Completed assembly of test bed with motor and ironless coreless electricity generator.	35
Figure 3.9	Three phase induction motor	36
Figure 3.10	Tachometer used to measure the rotational speed of the rotor.	37
Figure 3.11	Inverter used to convert direct current to alternating current	37
Figure 3.12	Oscilloscope to measure wave frequency and the voltage output	38
Figure 3.13	Wave frequency and the output voltage were produced by oscilloscope	39
Figure 3.14	DC electronic load used in the close circuit test	40
Figure 3.15	Rectifier used in the closed circuit test	40

Figure 4.1	Part warping and Collision on stator of Ironless Coreless Generator	43
Figure 4.2	The all 12 pieces of Coil assembly to Stator	44
Figure 4.3	Wobbling and Rubbing when rotating the shaft	45
Figure 4.4	The washer was added to solve the rubbing issue.	45
Figure 4.5	The concept of car tire balancing machine can be applied to fabricate the jig	46
Figure 4.6	Results from oscilloscope from various rotational speed	48
Figure 4.7	Output Voltage (V_{rms}) versus Rotational Speed (RPM) for Ironless Coreless Generator	49
Figure 4.8	The different amplitude each phase	54
Figure 4.9	Coiling process perform manually using special jig	55
Figure 4.10	Waveform not sinusoidal at certain rotational speed	56
Figure 4.11	Different types of probe. The probe with blue color can reach maximum 1000V and probe with black color only can reach maximum 300V	57
Figure 4.12	Power generated by ironless coreless electricity generator versus rotational speed graph	60
Figure 4.13	Waveform characteristic on closed circuit test.	61

UMP

LIST OF SYMBOLS



η	efficiency
f	Frequency
ω	Rotating speed of rotor in rad/s
B	Magnetic flux
I	Current
V	Voltage
R	Resistance
P	Power
p	Number of poles
N	Rotational speed of rotors in RPM

LIST OF ABBREVIATIONS

AC	Alternating Current
AFPM	Axial-flux permanent-magnet
CAD	Computer Aided Design
CNC	Computer Numerical Control
DC	Direct Current
emf	Electromotive Force
NdFeB	Neodymium Iron Boron
RMS	Root Mean Square
<i>rpm</i>	Revolution Per Minute
<i>N</i>	Rotational speed of rotors in RPM



UMP

CHAPTER 1

INTRODUCTION

1.1 Research Background

Magnetic material to be used as a magnetic core due to high magnetic permeability to guide the magnetic field in electrical, electromechanical and magnetic devices such as transformers, generators, electric motors and magnetic assemblies. Ferromagnetic metal such as iron, or ferrimagnetic compounds such as ferrites applied to make magnetic materials.

Ironcore lamination introduces to overcome solid core issued in a generator and to maximize the efficiency. Anyhow the ironcore lamination still gives the major drawback to the generator. Magnetic particles in the core tend to line up with the magnetic field of the permanent magnets, when the ironcore lamination is exposed to the magnetic field. The magnetic fields will change the direction when the magnets are rotated. This induces continuous movement of the ironcore magnetic particles in order for them to align with the change of magnetic field direction and coincidentally produces molecular friction. This in turn produces heat and is then distributed to the ironcore lamination and windings. Heat causes and increase in winding resistance and at the same time retains electromagnetism in the windings and ironcore laminations.

‘Cog’ also known as an attraction force between permanent magnets and ironcore lamination in a generator. The cog will reduce the inefficiency of the generator. The cog exist when the heat generated by rotation. The increasing of rotation, the more power is generated from generator, but the more power is required to maintain the rotation (Zhang et al., 2013; Ting & Yeh, 2014).

A lot of experiment and improvement have been done to reduce the cog and to increase the efficiency of generator (Kurt, Gör & Demirtaş, 2014). Most of researcher focusing to minimize the cogging effect and optimization on ironcore, but this problem still cannot avoid (Gor & Kurt, 2016). An effort made to remove iron core material from an electric motor was demonstrated with great success more than a decade ago. The success story of this ironless motor has been widely shared by both the researchers and players in the industries. The idea behind this achievement is removing the iron core lamination and replacing it with non-ferrous material. The ironless motor works flawlessly and one of the major advantages comes from its outstanding positional accuracy and repeatability due to no cogging affecting the positioning.

A similar idea may be applied to demonstrate coreless generator design. Effort made on this subject, however, is still lacking (Mahmoudi et al., 2013; Virtic & Avsec, 2011). The idea of removing ironcore lamination material may cause non-concentrated flux and lead to deterioration in output power efficiency (Ahmed & Ahmad, 2013). However, there is a method which may be used to concentrate and focus magnetic flux to create denser magnetic field. An additional permanent magnet arrangement added to the generator may be a solution to address this issue. The absence of ironcore lamination in the system also represents cog-free rotation. This provides advantage in terms of very low starting torque and less counter electromotive force is produced.

1.2 Research Objectives

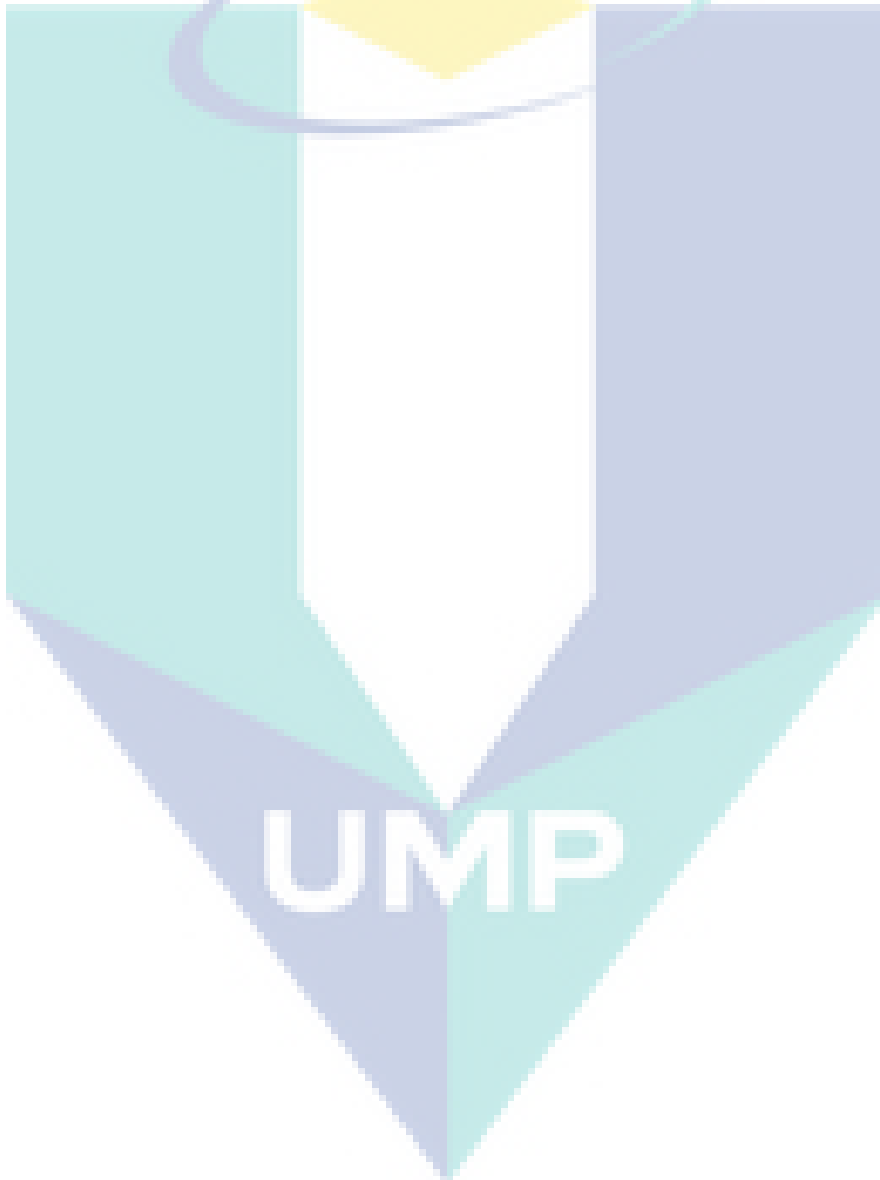
The present study sought to achieve the following objectives:

- To analyse output wave characteristic of the generator.
- To analyse no load and load speed performance of the generator.

1.3 Research Scope

The scope of the present research was limited to the following parameters:

- A generator producing $416V_{\text{rms}}$ at rotational speed of ~ 1800 RPM.
- Re-fabrication of axial flux permanent magnet generator (rotor & stator).
- Maximum voltage 160V for closed circuit test.



CHAPTER 2

LITERATURE REVIEW

2.1 Electricity Generation

Electricity generation is the operation of generating electric power from other sources of elemental energy. For electric utilities, it is the first process in the legal transfer of electricity to consumers. The other processes, electricity transmission, distribution, and electrical power storage and recovery using pumped-storage methods are usually taken out by the electric power industry. Electricity is most often brought forth at a power station by electromechanical generators, mainly driven by heat engines fuelled by burning or nuclear fission, but also by other means such as the kinetic energy of running water and wind. Other energy sources include solar photovoltaics and geothermal power.

Figure 2.1 Electricity Transportation.

The underlying rules of electricity generation were exposed during the 1820s and early 1830s by the British scientist Michael Faraday. This method is even practiced today: electricity is brought forth by the motion of a loop of wire, or a disc of copper between the poles of a magnet.



Figure 2.1 Electricity Transportation

2.1.1 Magnetic Field

A magnetic field is the magnetic effect of electric currents and magnetic materials. A magnetic field can be represented by lines of force, which is a concept connected to Faraday's law. The strength of the magnetic field can be visualized by observing the density of these lines. Figure 2.2 shows the comparison of the density of lines between weaker and stronger magnetic fields. The magnetic field is stronger if the magnetic strength of the magnet is stronger.

UMP

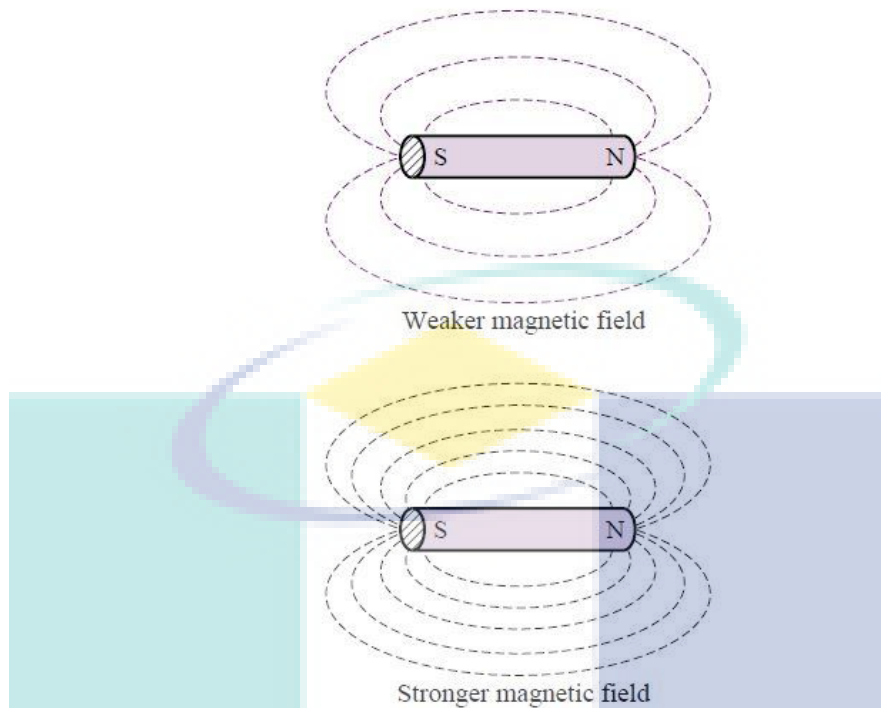


Figure 2.2 Figure shows the differences in line density in weaker and stronger magnetic fields

Another familiar source of magnetic fields is the current-carrying wire. In Figure 2.3, show the magnetic field associated with an infinitely long current-carrying wire. The magnetic field is wrapped in circles about the wire, with the direction of the rotation of the circles determined by the right hand rule (if the thumb of your right hand is in the direction of the current, your fingers will curl in the direction of the magnetic field).

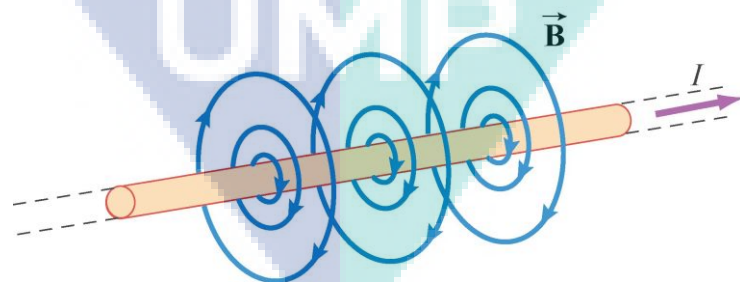


Figure 2.3 Magnetic field lines due to an infinite wire carrying current I .

2.1.2 Concept Regarding Magnetic Field Cutting

Based on Fleming's right-hand rule, when a wire moves through a magnetic field at a velocity, a certain amount of voltage can be generated. The generated voltage is opposite with the current generated based on Fleming's left-hand rule. Figure 2.4 shows the usage of Fleming's left-hand rule on the magnetic field where F is the force acting on the wire, B is the flux density and I is the current produced while Figure 2.5 shows the usage of Fleming's right-hand rule on the magnetic field where e is the generated voltage or also called counter electromotive force, B is the magnetic flux while v is the velocity of wire.

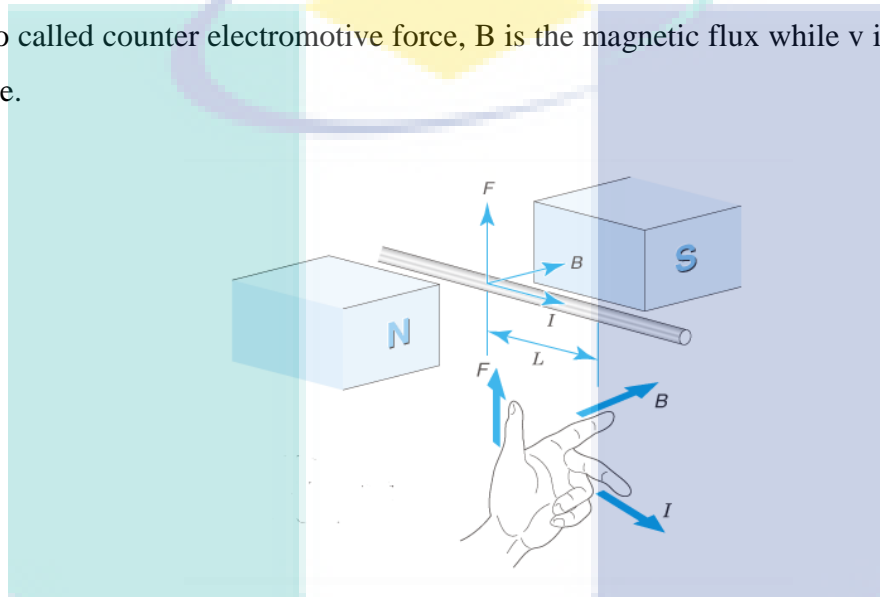


Figure 2.4 Fleming's left-hand rule on magnetic field

UMP

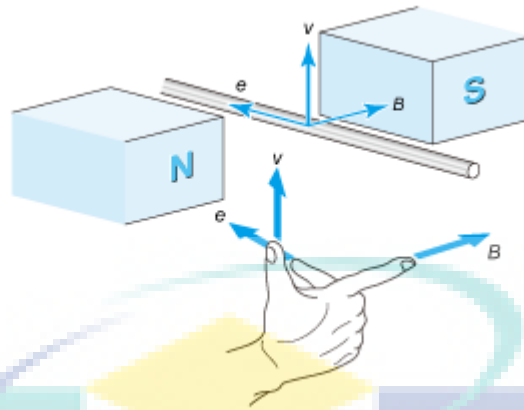


Figure 2.5 Fleming's right-hand rule on magnetic field

Since the generated voltage function is to reduce the current, it is also called the counter electromotive force. The velocity, v , can be expressed as in Eq. 2.1. The counter electromotive force that has been generated in the wire is expressed in Eq. 2.2.:

$$v = \omega R \quad (2.1)$$

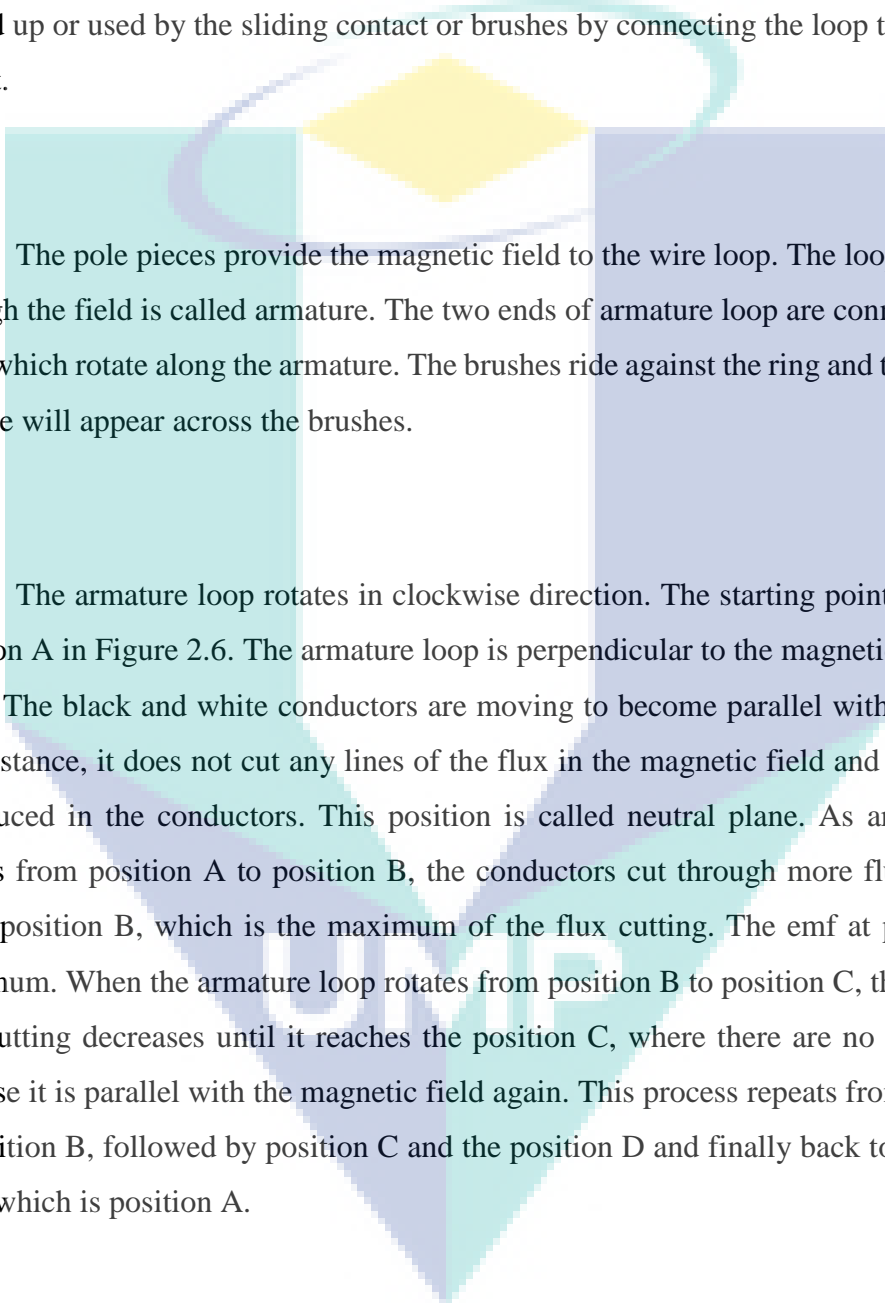
$$e = BLR\omega \quad (2.2)$$

Where v is the velocity of the wire, ω is the rotating speed of rotor in radian per second, and R is the turning radius in metre. From equation 2.2, the counter electromotive force is proportional to the rotating speed ω .

2.2 Ironcore Electricity Generator

2.2.1 Element and Working Principle

An electricity generator consists of a wire loop that can be rotated in a stationary magnetic field and thus, induced emf is produced in the loop. The induced emf will be picked up or used by the sliding contact or brushes by connecting the loop to an external circuit.



The pole pieces provide the magnetic field to the wire loop. The loop that rotates through the field is called armature. The two ends of armature loop are connected to slip rings which rotate along the armature. The brushes ride against the ring and the generated voltage will appear across the brushes.

The armature loop rotates in clockwise direction. The starting point is shown as position A in Figure 2.6. The armature loop is perpendicular to the magnetic field at this point. The black and white conductors are moving to become parallel with the field. In this instance, it does not cut any lines of the flux in the magnetic field and thus, no emf is induced in the conductors. This position is called neutral plane. As armature loop rotates from position A to position B, the conductors cut through more flux until they reach position B, which is the maximum of the flux cutting. The emf at position B is maximum. When the armature loop rotates from position B to position C, the number of flux cutting decreases until it reaches the position C, where there are no flux cuttings because it is parallel with the magnetic field again. This process repeats from position A to position B, followed by position C and the position D and finally back to the original point which is position A.

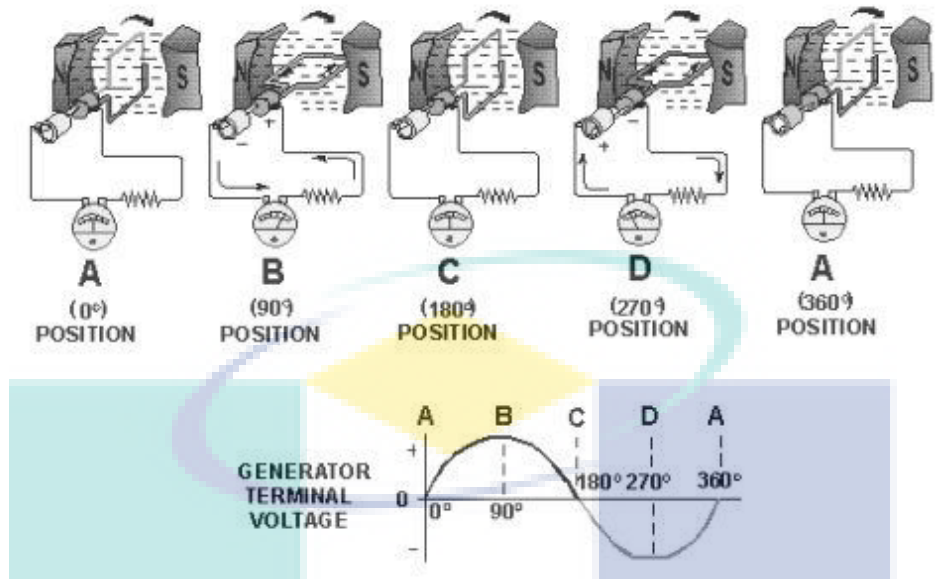


Figure 2.6 Illustration shows the various position of armature as well as generator terminal voltage in various position of armature

Spinning a wire loop within a uniform magnetic field induces a voltage between the loop terminals. If the loop terminals are connected with an electrical load, a current will be produced in the circuit. The current generated by a basic electrical generator is alternating current. If the generator is intended to supply direct current, it must have a collector, which is a device working as a mechanical rectifier (Portela, Sepúlveda, & Esteves, 2008).

UMP

2.2.2 Attraction between Ironcore Lamination and Permanent Magnets

The iron core as well as the permanent magnets used in the iron core generator carries important roles in making the iron core electricity generator functional. Because of the attraction between the iron core lamination and the permanent magnets, it makes the iron core electricity generator become less efficient. Based on the design of the iron core electricity generator, the cogging effect is always present within the generator itself. It is because the force between the permanent magnets and the iron core lamination stack of the iron core electricity generator causes not only the attraction force between themselves, but also a force in the direction of motion as well. This type of force depends on the relative position of the laminated teeth with regards to the magnetic poles for the iron core electricity generator (Stampfi, 2003).

2.2.3 Cogging Torque in An Ironcore Generator

The cogging torque may also be referred to as reluctance torque due to the reluctance variation that exists in the tooth and slot of the magnet current source (Mosincat, Lu & Pedersen, 2011). Cogging torque as high as 25% of the rated torque can result due to the improper design of the machines (Krishnan, 2009).

Choosing the right angle of clearance at the both ends will help to reduce the cogging effects within the iron core generator. Nevertheless, ironless configuration will be the right solution for high smoothness of motion. This is because the ironless configuration has no cogging effect since it has no iron moving parts at all (Stampfi, 2003). Other techniques such as varying the magnet strength used on the generator, varying the magnet arc length, the slot width, and the radial shoe depth as well as using fractional slots per pole, can be used to minimize the cogging torque of the generator (Krishnan, 2009; Bianchi & Bolognani, 2002). Almost all techniques that are used to reduce the cogging torque also reduce the counter-electromotive force and thus, reduce the resultant running torque (Mosincat, Lu & Pedersen, 2011).

2.3 Ironless Coreless Generator

The iron cored generator is a type of the generator that widely used in the marketplace. The usage of ferrite material on the iron-cored generator makes the generator itself become less efficient because of its high starting and cogging torques. The coreless electricity generator, the redesigning of the iron-cored generator by minimizing the usage of ferrite material on the generator itself, is seen as a promising solution to capture energy during in motion. Compare to the iron-cored electricity generator, coreless electricity generator had much lower cogging torque because of the elimination of the most ferrite material within the generator itself.

However, compare to the ironless electricity generator, it has much lower starting torque, higher efficiency and can produce a considerable amount of electricity based on the size of the generator itself. This type of generator has no cogging effect and low CEMF resistance during the operation to produce the electricity. It is because the generator itself does not have the iron core lamination that can be found in the iron-cored and coreless electricity generator. The iron-cored used in the cored system causes magnetic field between the iron-cored and the permanent magnet to resist the motion and thus, increase the starting torque and cause unnecessary loss of the electricity generated. The ironless electricity generator, the design that eliminate the usage of ferrite on the generator can further decrease the starting torque and unnecessary losses. From there, the ironless electricity generator is a promising solution to overcome issues faced by the iron-cored generator.

2.3.1 Axial Flux Permanent Magnet

Axial permanent-magnet (AFPM) machines are being developed for many applications due to their attractive features. They are usually more efficient because the losses of field excitation are eliminated, resulting in significant rotor loss reduction. AFPM machines with coreless stators are regarded as high-efficiency machines for distributed power generation systems. In these machines, the core losses of stators are eliminated. In addition, the ironless stator eliminates the direct magnetic attraction between rotors and stators. These machines have long diameters compared to short lengths and hence the capability of producing high torques.

The disk-shape profile of a generator makes it compact and particularly suitable for mechanical integration with wind turbines. Despite the absence of stator iron, rare-earth magnets on the rotors are able to create a working flux density of about 0.3 T at the winding.

The advantage of implementing a disk permanent-magnet synchronous generator in a wind turbine is to eliminate gearbox, which is necessary for conventional generators. Due to centrifugal forces tending to move magnets from its places, the use of AFPM machines is generally limited to low-speed applications (for example in direct coupled wind turbine).

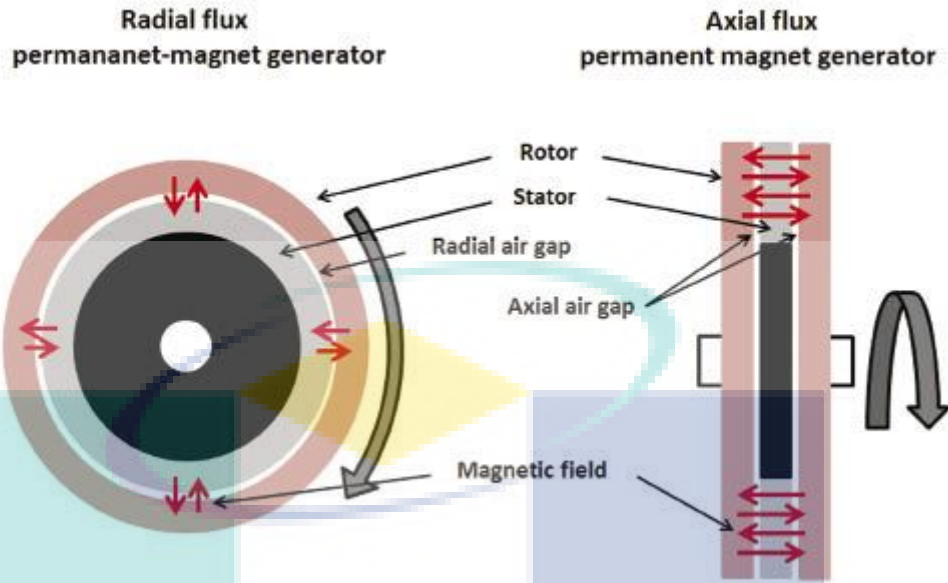


Figure 2.7 Differences between Radial Flux Permanent Magnet Generator and Axial Flux Permanent Magnet Generator

2.3.2 Structure of Axial Flux Permanent Magnet

Axial flux permanent magnet consist two outer rotor disks and one coreless stator in between. The rectangular flat-shaped high-energy Nd-Fe-B magnets are glued onto inner surfaces of two rotor disks. It also can be designed fit into slot on the rotor and cover by plate or without plate. It prefer to cover by plate to avoid the magnet pull out from stator. The rotor poles with an opposite arrangement (N-S type) are shown in Figure 2.8.

UMP

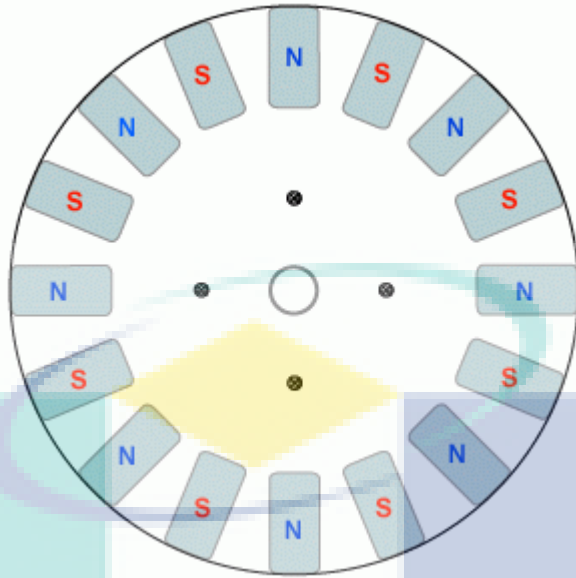


Figure 2.8 The arrangement magnets on the rotor (N-S type)

The arrangement of the copper winding (see Figure 2.9) should be designed well so that maximum magnetic flux cutting can be done which maximizes the efficiency of the generator itself. For the coreless electricity generator, coils of wire are used instead of multiple interconnected wires where the magnet rotates over them to produce the electricity. For instance, when the north pole of a magnet passes through a coil, the current flows in one direction, and when the south pole passes over the coil, current flows through in the opposite direction. The most electricity is generated while the magnetic field is at 90 degrees to the coil winding and no electricity is generated when the magnetic field is parallel to the coil.

UMP

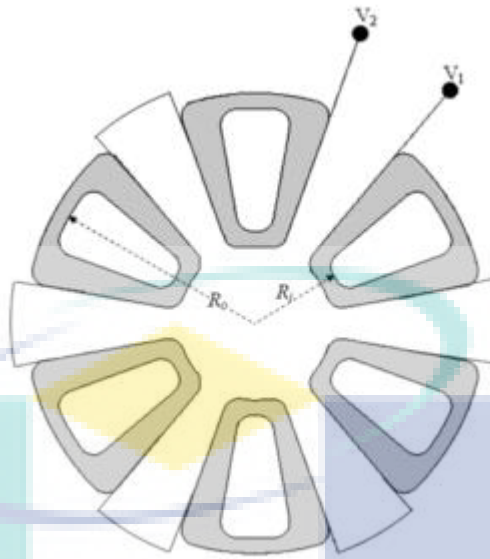


Figure 2.9 Example of coil winding of one phase in a 12-pole pair AFPM machine with single –layer trapezoidal windings.

2.3.3 Types of magnet in Ironless Coreless Generator

Magnets are objects that generate a magnetic discipline, a force field that either attracts or repels certain materials, such as nickel and iron. Permanent magnets are magnets retain their magnetism once magnetized. On that point are typically four categories of permanent magnets: neodymium iron boron (NdFeB), samarium cobalt (SmCo), alnico, and ceramic or ferrite magnets.

The process of choosing magnet quit critical since the magnet meets the important function to ensure generator efficiency is to comprehend. Later all the factors studied, the best magnet to be used are Neodymium Iron Boron (NdFeB) magnet. The Neodymium Iron Boron (NdFeB) magnet, provide the greatest opportunity to the automotive sector since the continuous advance in the new high magnetic field rare-earth permanent magnets (Mo et al., 2008). The primary ingredient in manufacturing is how to decrease the monetary value, the Neodymium Iron Boron (NdFeB) magnet easily available in the market and cost efficiencies make rapid permanent magnet generator development (Chan & Lai, 2007). This modern magnetic material can easily be obtained in the securities industry with different patterns and forms, thus the purpose of the usage of these magnets

can be managed well. It can supply power even during electrical network failure as an upshot of the built-in permanent self-excitation (Drazikowski & Włodzimierz, 2011).

For large-pole number, the diameter of the magnets and coils are fixed and limit the radial length of the active area, which makes the generator have large radius but small active length. Equally for the small-pole number, low-power turbines tend to spin relatively fast, but as power increases and a diminution in speed is required, the number of poles should increase, which can produce the radial length of the active area become small compared to the radius of the stator. This kind of problem can be reduced by using trapezoidal or rectangular magnets whereby this helps the pole pitch and active length can be decoupled from each other (Bumby & Martin, 2005).

2.3.4 Coil Design for the Ironless Coreless Generator

To maximize the efficiency of the generator, copper winding arrangements should be designed well so that maximum magnetic flux cutting can be done. Coils of wire applied instead of multiple interconnected wires for the coreless electricity generator, where the magnet rotates over them to generate the electricity. For instance, when the north pole of a magnet passes through a coil, the current flows in one direction, and when the south pole passes over the coil, current flows through in the opposite direction. Basically, while magnetic field at 90 degrees to the coil winding the electricity is generated and when the magnetic field is parallel to the coil no electricity is generated.

The magnet at the north pole pushes upward on the left radial leg of the coil and at the same time, the magnet at the south pole is pushing downward on the right radial leg. These two clockwise motions cause the electricity being generated. Notice that if both radial legs are pushing in the same direction, for example, the left and right radial leg are pushing upward together at the same time, the motion cancels out each other and thus, no electricity is generated. That is the reason which shows that it is essential to arrange the magnet poles alternatively so that the motion will not cancel out each other.

The size of the copper winding is also an important criterion for the efficiency of coreless electricity generator. Figure 2.10 shows the coil dimension for the axial-flux permanent magnet generator where c represents the thickness of the coil and $d(r)$ is the diameter of the coil.

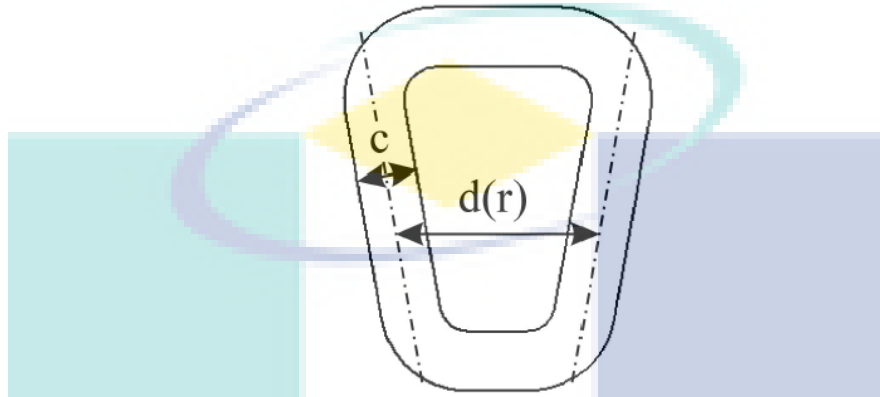


Figure 2.10 Coil dimension for the axial-flux permanent magnet generator

The pole pitch and diameter of coil can be calculated via Eq. 2.3 and Eq. 2.4 respectively where τ is pole pitch, r is radius, k is the number of coils per phase, n is the rotor rotation speed in rpm, l is the length of conducting wire, z is the number of turns, c is the coil thickness, d is the coil diameter as shown in Figure 2.10, while x is the actual position in mm and E is the electromotive force. In order to make pole pitch equal to diameter of coil, the thickness of the coil cannot be increased more than 33% of pole pitch because of geometrical relation. In other words, the distance between the coils must be equal to 133% of the pole pitch (Drazikowski & Włodzimierz, 2011). Figure 2.11 shows the approximated power of the generator via the different relative thickness of coil (c/τ) in Drazikowski and Włodzimierz's (2011) research.

$$\tau = 2r \sin(7.5^\circ) \quad (2.3)$$

$$E(x) = k \frac{2\pi r \cdot n}{60} l z \frac{1}{c} \left[\int_{x-\frac{1}{2c}}^{x+\frac{1}{2c}} B_m \sin\left(\frac{\pi}{\tau} x\right) dx - \int_{x-\frac{1}{2c}}^{x+\frac{1}{2c}} B_m \sin\left(\frac{\pi}{\tau} (x+d)\right) dx \right] \quad (2.4)$$

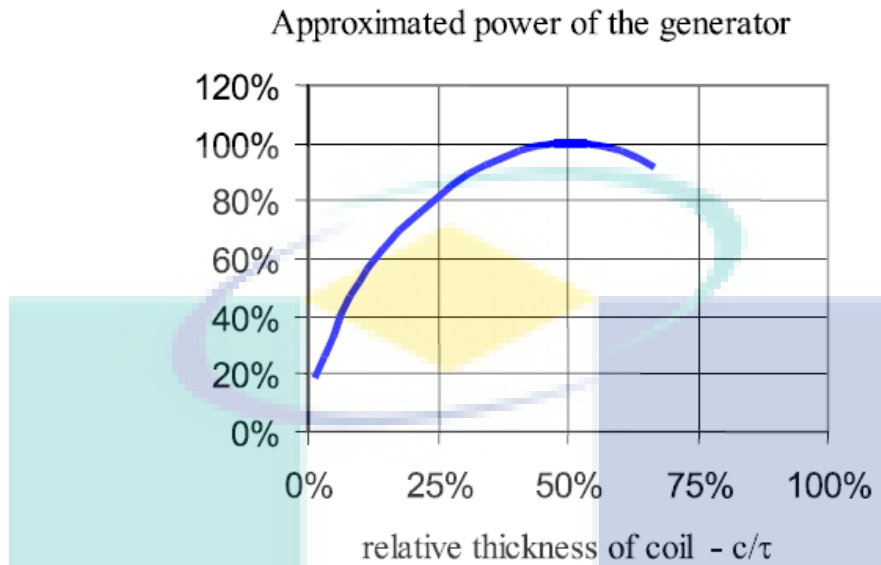


Figure 2.11 Approximated power of the generator via the different relative thickness of coil (c/τ)

2.3.5 Gap Distance between Magnets

Some other criteria need to take care is the gap distance between magnets of the coreless generator. The efficiency of the generator not the optimum level if the gaps between magnets too far. However, if the gaps between the magnets are too close to each other, there will be no room or space left to place the stator (copper coil winding) between them.

The optimum air-gap size is calculated using Eq. 2.6, where B_m represents maximum flux density in the air-gap, g represents the thickness of magnet, μ_0 represents air permeability that can be calculated using Eq. 2.5, B_r is for remanence, H_c is for coercivity of magnet, δ represents air-gap length, H is for external magnetic field strength and m represents magnetic moment (Drazikowski & Włodzimierz, 2011).

$$\mu_0 = 4\pi \cdot 10^{-7} \frac{H}{m} \quad (2.5)$$

$$B_m = \frac{2g\mu_0 B_r H_c}{B_r \delta + 2g\mu_0 H_c} \quad (2.6)$$

The graph power of the generator versus air gap distance shown the optimum air gap size is around 35mm (see Figure 2.12). However the air gap distance between 33mm to 38mm shown approximately same output power. For manufacture easy to control the tolerance around 5mm (Drazikowski and Włodzimierz's (2011)).

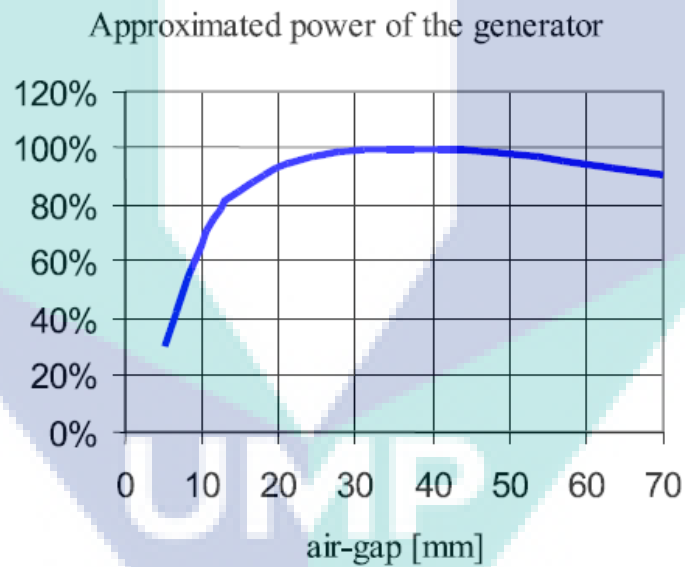


Figure 2.12 Approximated power of the generator varies on air-gap distance

2.3.6 Number of Poles and Coils for the Ironless Coreless Generator

There are a few sets of rules for the pole and slot combinations that make non-overlap windings valid as suggested by Gieras, Wang and Kamper (2008). The rules are:

- The number of poles must be even;
- The number of slots must be a multiple of the number of phases and must be even in the case of single layer windings;
- The number of coils and slots are equal in double layer windings; in single layer windings the number of coils is equal to half the number of slots;
- The number of coils in a coil group must be an integer;
- The number of slots cannot be equal to the number of poles.

To verify the number of poles, Eq. 2.7 is used to perform such function, as N represents rotational speeds of the rotors in RPM, f represents frequency of the rotors and p represents number of poles on each rotor (Rizzoni, 2007).

$$N = \frac{120f}{p} \quad (2.7)$$

2.4 Electrical Waveform

2.4.1 Waveform Characteristic

Electrical Waveforms are basically visual representations of the variation of a voltage or current over time. There are many different types of electrical waveforms available but generally they can all be broken down into two distinctive groups;

a) Uni-directional Waveforms

These electrical waveforms are always positive or negative in nature flowing in one forward direction only as they do not cross the zero axis point. Common uni-directional waveforms include Square-wave timing signals, Clock pulses and Trigger pulses.

b) Bi-directional Waveforms

These electrical waveforms are also called alternating waveforms as they alternate from a positive direction to a negative direction constantly crossing the zero axis point. Bi-directional waveforms go through periodic changes in amplitude, with the most common by far being the Sine-wave.

Whether the waveform is uni-directional, bi-directional, periodic, non-periodic, symmetrical, non-symmetrical, simple or complex, all electrical waveforms include the following three common characteristics:

a) Period

This is the length of time in seconds that the waveform takes to repeat itself from start to finish. This value can also be called the Periodic Time, (T) of the waveform for sine waves, or the Pulse Width for square waves.

b) Frequency

This is the number of times the waveform repeats itself within a one second time period. Frequency is the reciprocal of the time period, ($f = 1/T$) with the standard unit of frequency being the Hertz, (Hz).

c) Amplitude

This is the magnitude or intensity of the signal waveform measured in volts or amps.

2.4.2 Periodic Waveforms

Periodic waveforms are the most common of all the electrical waveforms as it includes Sine Waves. The AC (Alternating Current) mains waveform in your home is a sine wave and one which constantly alternates between a maximum value and a minimum value over time.

The amount of time it takes between each individual repetition or cycle of a sinusoidal waveform is known as its “periodic time” or simply the Period of the waveform. In other words, the time it takes for the waveform to repeat itself.

Then this period can vary with each waveform from fractions of a second to thousands of seconds as it depends upon the frequency of the waveform. For example, a sinusoidal waveform which takes one second to complete its cycle will have a periodic time of one second. Likewise a sine wave which takes five seconds to complete will have a periodic time of five seconds and so on.

So, if the length of time it takes for the waveform to complete one full pattern or cycle before it repeats itself is known as the “period of the wave” and is measured in seconds, we can then express the waveform as a period number per second denoted by the letter T.

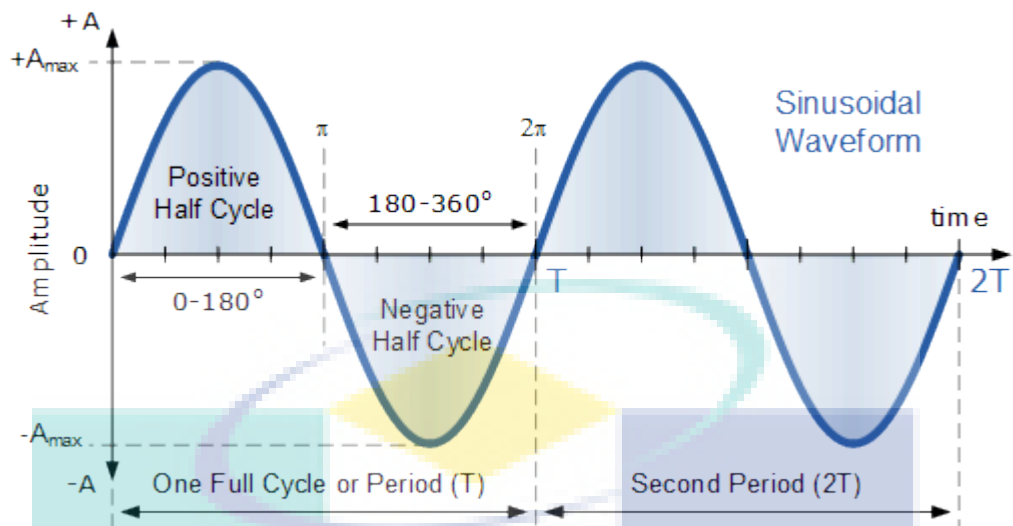


Figure 2.13 A sine wave waveform

For sine wave waveforms only, the periodic time of the waveform in either degrees or radians, as one full cycle is equal to 360° ($T = 360^\circ$) or in Radians as 2π , 2π ($T = 2\pi$), then 2π radians = 360° .

The time it takes for electrical waveforms to repeat themselves is known as the periodic time or period which represents a fixed amount of time. If take the reciprocal of the period, ($1/T$) end up with a value that denotes the number of times a period or cycle repeats itself in one second or cycles per second, and this is commonly known as Frequency with units of Hertz, (Hz). Then Hertz can also be defined as “cycles per second” (cps) and 1Hz is exactly equal to 1 cycle per second.

Both period and frequency are mathematical reciprocals of each other and as the periodic time of the waveform decreases, its frequency increases and vice versa with the relationship between Periodic time and Frequency given as.

2.4.3 Ripple on Electrical Waveform

The most common meaning of ripple in electrical science is the small unwanted residual periodic variation of the direct current (DC) output of a power supply which has been derived from an alternating current (AC) source. This ripple is due to incomplete suppression of the alternating waveform within the power supply.

Ripple factor (γ) may be defined as the ratio of the root mean square (rms) value of the ripple voltage to the absolute value of the DC component of the output voltage, usually expressed as a percentage. However, ripple voltage is also commonly expressed as the peak-to-peak value. This is largely because peak-to-peak is both easier to measure on an oscilloscope and is simpler to calculate theoretically. Filter circuits intended for the reduction of ripple are usually called smoothing circuits.

The simplest scenario in AC to DC conversion is a rectifier without any smoothing circuitry at all. The ripple voltage is very large in this situation; the peak-to-peak ripple voltage is equal to the peak AC voltage. A more common arrangement is to allow the rectifier to work into a large smoothing capacitor which acts as a reservoir. After a peak in output voltage the capacitor (C) supplies the current to the load (R) and continues to do so until the capacitor voltage has fallen to the value of the now rising next half-cycle of rectified voltage. At that point the rectifiers turn on again and deliver current to the reservoir until peak voltage is again reached. If the time constant, CR, is large in comparison to the period of the AC waveform, then a reasonably accurate approximation can be made by assuming that the capacitor voltage falls linearly.

A further useful assumption can be made if the ripple is small compared to the DC voltage. In this case the phase angle through which the rectifiers conduct will be small and it can be assumed that the capacitor is discharging all the way from one peak to the next with little loss of accuracy.

Another approach to reducing ripple is to use a series choke. A choke has a filtering action and consequently produces a smoother waveform with less high-order harmonics. Against this, the DC output is close to the average input voltage as opposed to the higher voltage with the reservoir capacitor which is close to the peak input voltage.

Ripple is undesirable in many electronic applications for a variety of reasons:

- The ripple frequency and its harmonics are within the audio band and will therefore be audible on equipment such as radio receivers, equipment for playing recordings and professional studio equipment.
- The ripple frequency is within television video bandwidth. Analogue TV receivers will exhibit a pattern of moving wavy lines if too much ripple is present.
- The presence of ripple can reduce the resolution of electronic test and measurement instruments. On an oscilloscope it will manifest itself as a visible pattern on screen.
- Within digital circuits, it reduces the threshold, as does any form of supply rail noise, at which logic circuits give incorrect outputs and data is corrupted.
- High-amplitude ripple currents shorten the life of electrolytic capacitors

CHAPTER 3

METHODOLOGY

3.1 Introduction

The development works were divided into two stages, namely, the development works for the ironless electricity generator and the development works on the test bed to test the ironless electricity generator. Most of the fabrication works used CNC machine to produce the real model of the ironless coreless electricity generator. All the parts were assembled using mechanical screw and bolt after all the parts were ready for assembly. Figure 3.1 shown the flow chart for Ironless Coreless Generator.

UMP

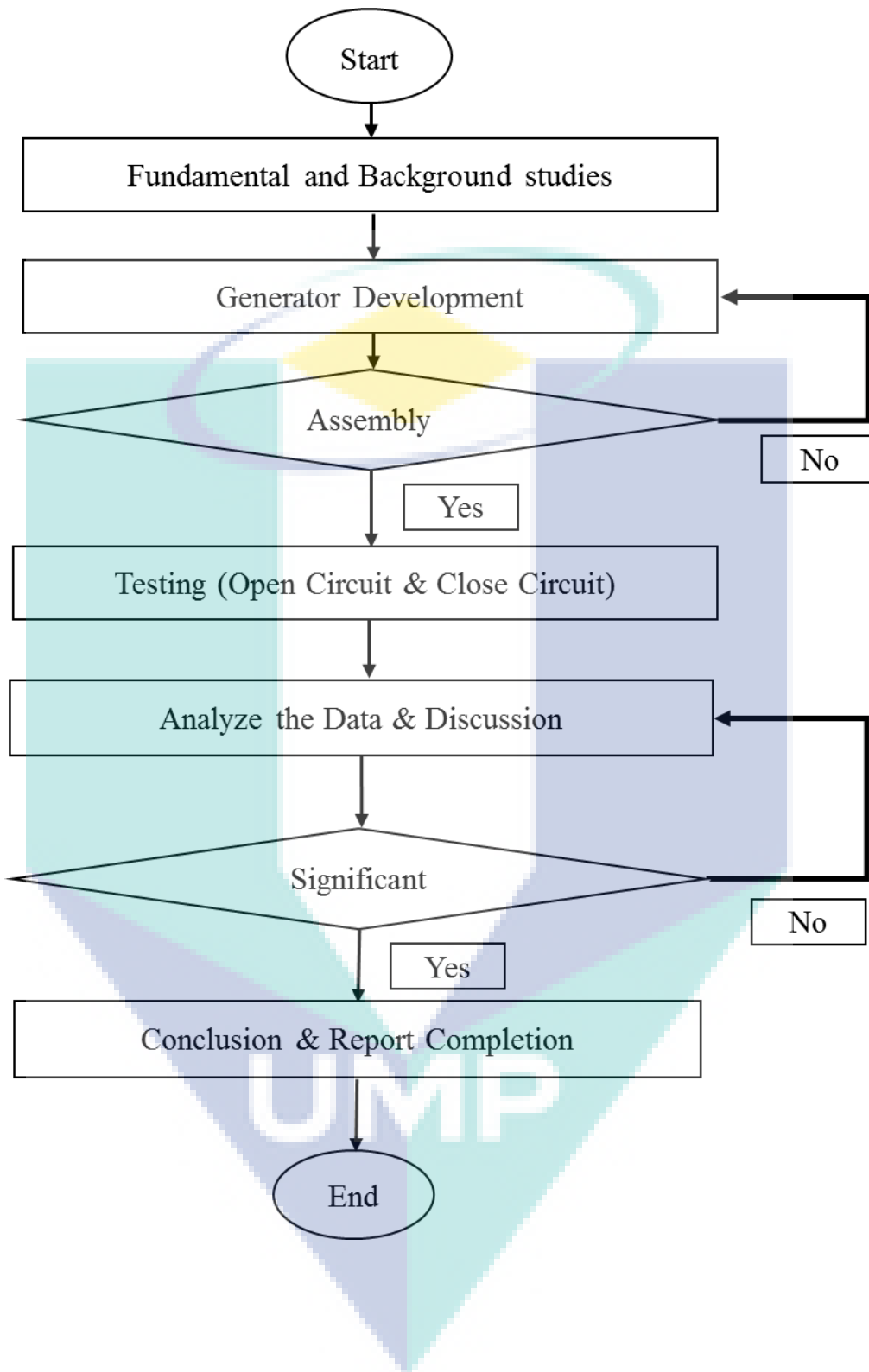


Figure 3.1 Flow chart for Ironless Coreless Generator

3.2 Fabrication Rotor and Stator for the Ironless Coreless Electricity Generator

The fabrication for replacement the rotor and stator using CNC Milling Machine. In the Catia V5R21 software, the machining sequence, tool used and cutting parameter were set accordingly.

CAD (Computer Aided Design) file retrieved from software Solidworks has been convert to .stp or .igs to ensure Catia V5R21 Software able to read this drawing. After Catia V5R21 software read the drawing, the machining using CAM (Computer Aided Machining) has been perform. Roughing, profile contouring, drilling, spiral, z level function used to do a machining process. The cutting parameter like spindle speed, feedrate for machining, feedrate for approach and retract, depth of cut, stepover, cutting tool used, approach and retract were set accordingly. Simulation on Catia V5R21 software to verify no collision on part happen. After simulation is done, NC (Numerical Control) code is generate to unable CNC Machine read the code.

The machining material, plastic, was then accurately clamped on the machining bed of the CNC machine, followed by the zero position setting for the machining parts. When all was ready, the machining process began. The coolant must be ensured to have been sprayed on the tip of the cutting tools. This was necessary to make sure that the cutting tools were cold and prevented the tools from overheating. If the cutting tools became overheated, they could become spoiled and cause the machining process to fail. Figure 3.2 illustrate the process flow for machining process.

After the machining process and the finishing process were done, the completed machining parts were taken out and the trimming process began. To cut the machining parts out from the big plastic plate, handsaw was used. Later, the parts that were cut from the big plastic plate proceeded to the finishing trimming. Because parts were made on plastic, the excessive parts could use the plastic cutter for trimming. Figure 3.3, Figure

3.4 and Figure 3.5 illustrate the CNC Milling Machine used for fabrication, fabricated rotor and fabricated stator, respectively.

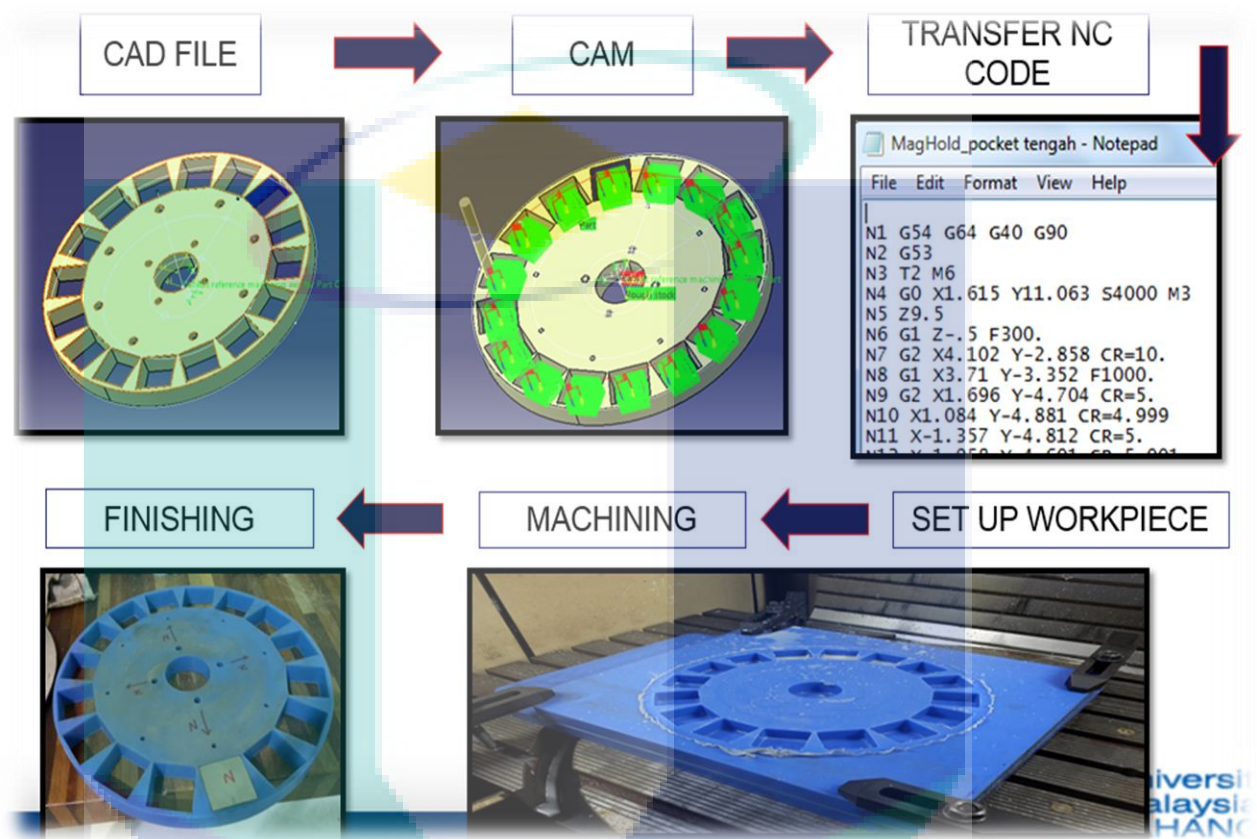


Figure 3.2 Process flow for machining process

UMP



Figure 3.3 Fabrication using CNC Milling Machine

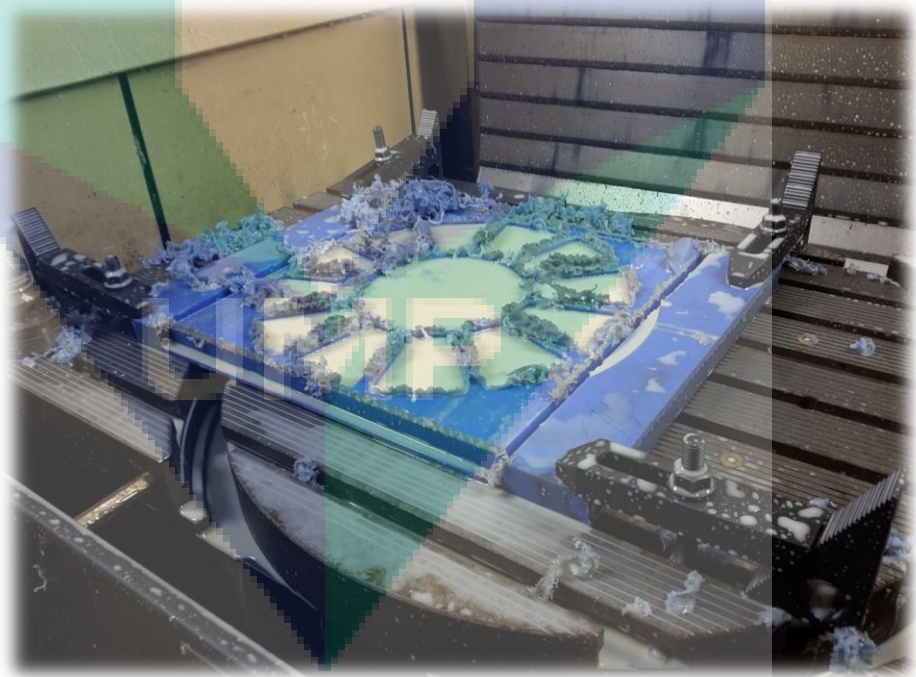


Figure 3.4 Fabrication Stator

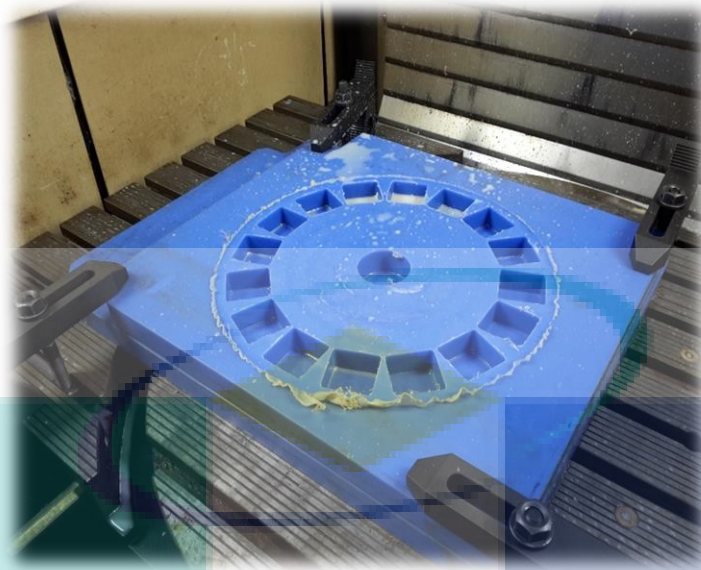


Figure 3.5 Fabrication Rotor

3.3 Assembly Magnet to Rotor

Magnets were the vital parts for this research. Without the magnets, no electricity could be generated in this research. The shipment of magnets came in bulk. To assemble the magnets into the rotor, the first step was to disassemble the magnet bulk into single quantities. Since the Neodymium magnet was so strong that could not be removed by using bare hand. The special jig used to perform such task used shear force to separate single unit of Neodymium magnet from the bulk.

After disassembling the magnets from the bulk into single quantities, the magnets were then pushed into the rotor by using mallet. The assembly process was carried out pole by pole. For example, the north pole was firstly assembles on stator and after all was done on the north pole, the assembly for the south pole was then carried out. By using a compass, the poles for the magnet could be easily identified. Figure 3.6 indicates the magnet assembly process into the rotor.



Figure 3.6 Magnet assembled into rotor

3.4 Assembly Ironless Coreless Generator

After all the parts of ironless coreless electricity generator were assembled, next was the assembly process for the generator. Firstly, the shaft support was pressed into the rotor. A few units of screw were placed without tightening them to ensure the position for shaft support and rotor would be aligned. After that, stator was placed between the rotors and the shaft support was pressed into the second rotor.

For the support plate, the bearing was pushed into the designated space on the side support plate and at the bottom so that both of the support plates were locked with top bottom support plate. Then, the shaft was connected through the support plate, the rotor and the shaft support. After the stator was aligned in the middle, the top plate was screwed to keep it locked. Figure 3.7 illustrates the sequence process to assemble the finished prototype of the ironless coreless electricity generator.

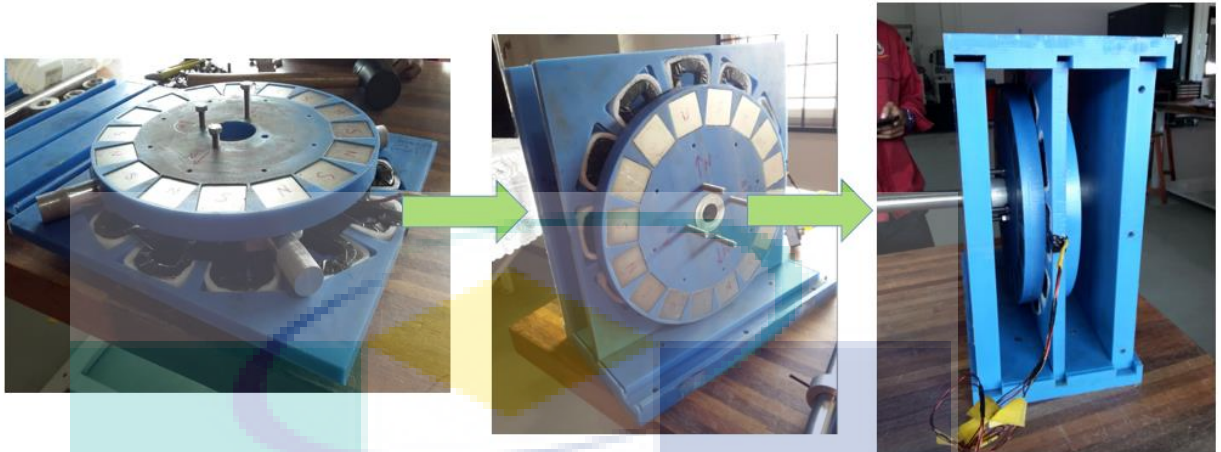


Figure 3.7 Sequence process for assemble prototype ironless coreless generator

After done assemble the ironless coreless generator, the next step is to assemble this generator to test bed. The test bed consisted of the bottom plate which had adjustable height mounting to cause the motor to spin the ironless coreless electricity generator. The motor mounting height had to be adjustable because with this function, the motor or prime mover could be aligned horizontally and accurately with less worry of having to redo the machining on the test bed required. After the alignment of the motor or prime mover was done, the bolt and nuts on the four corners of each screw were tightened to ensure the stiffness of the motor support.

The ironless coreless electricity generator was placed on the other side of mounting placement. The ironless coreless electricity generator was able to move horizontally before it was tightened in its place. This was to ensure that the connection in the motor or prime mover was secured in its place. After the shaft was horizontally aligned with the motor, a specially made connector was used to tighten the shaft connection between the motor and the ironless coreless electricity generator. Figure 3.8 shows the completed assembly of test bed with motor and ironless coreless electricity generator.

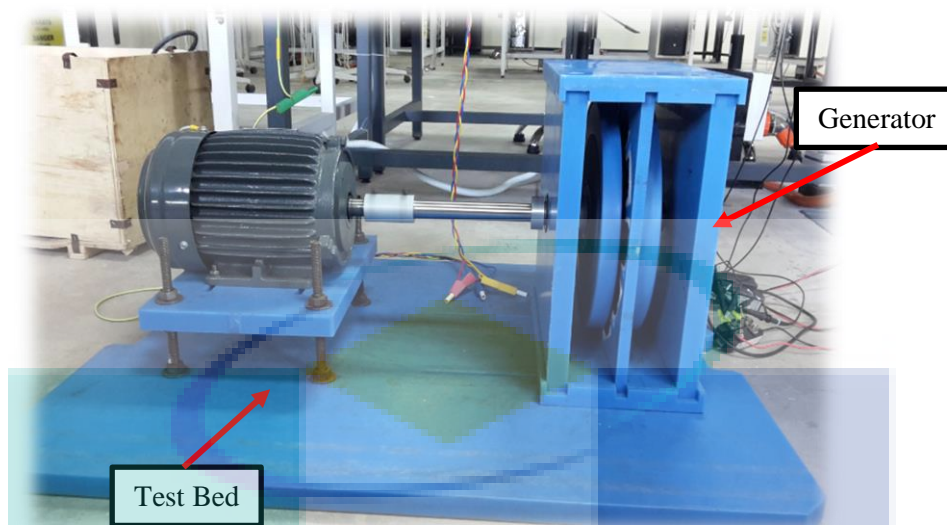


Figure 3.8 Completed assembly of test bed with motor and ironless coreless electricity generator.

3.5 Open Circuit Test on Ironless Coreless Electricity Generator

In the open circuit test for the ironless coreless electricity generator, a 2-horsepower three-phase induction motor was used to function as the prime mover to rotate the rotor of the generator. This induction motor had a rating no-load rotational speed of 1400RPM, input voltage of 220V to 240V for delta connection, input voltage of 380V to 415V for star connection, rating current of 5.64A to 6.15A for delta connection and rating current of 3.26A to 3.56A for star connection with efficiency of 75.5% if the load usage was below half of the motor but 78.5% if the load usage was above three quarters of the motor. Figure 3.9 shows the three phase induction motor.



Figure 3.9 Three phase induction motor

Since the motor was using alternating current supply to power up, the inverter was used to convert the direct current supply into alternating current supply so that the motor was able to operate. The inverter had an efficiency of 96% when working within the rated load. Wires were used to connect the power source to the inverter. They were also used to connect the inverter to the motor. To measure the wave frequency and the voltage output of the three-phase circuit of the ironless coreless electricity generator, the oscilloscope was used. The oscilloscope was connected to the end of the three-phase circuit by using wires. The tachometer was used to measure the rotational speed of the rotors of the generator. Figure 3.10 illustrates the tachometer used to measure the rotational speed of the rotor. Figure 3.11 shows the inverter used in the open circuit test. Figure 3.12 shows oscilloscope to measure wave frequency and the voltage output.

UMP



Figure 3.10 Tachometer used to measure the rotational speed of the rotor.



Figure 3.11 Inverter used to convert direct current to alternating current



Figure 3.12 Oscilloscope to measure wave frequency and the voltage output

The three-phase induction motor was connected using star connection as it could support higher voltage. The inverter was connected to power supply and the motor after the ironless coreless electricity generator and the motor were in place. The three-phase circuit of the ironless coreless electricity generator was then connected to the oscilloscope. When all the mechanical assembly and electrical assembly were done, the experiment began. After the power supply was switched on, a specified amount of power transferred to the motor was set by the inverter. The input power of the motor was controlled by the inverter using frequency input in the inverter. Once the setting was done and the rotational speed of the rotor was stabilized, the rotational speed of the rotor was observed using tachometer and recorded. To clearly obtain the graphical output wavelength from the oscilloscope, the x-axis was set to 10 milliseconds per column and y-axis was set to 20V or 50V per row, depending on the output voltage of the experiment. When the rotors were rotating, wave frequency and the output voltage were produced (see Figure 3.13). When everything was observed to have been completed, screenshots of the oscilloscope were taken and the data were transferred into the computer for data extraction process.

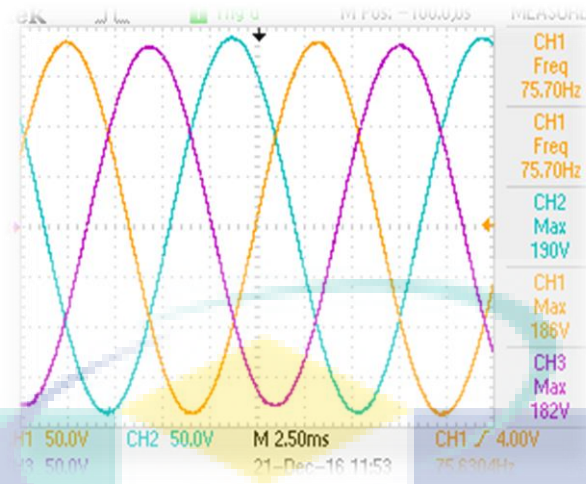


Figure 3.13 Wave frequency and the output voltage were produced by oscilloscope

3.6 Closed Circuit Test on Ironless Coreless Electricity Generator

After the open circuit test was done, the closed circuit test or loaded test was performed to test the ironless coreless electricity generator. The reason to perform the closed circuit test was to experiment the capabilities of the fabricated ironless coreless electricity generator under loaded conditions. In the closed circuit test, the generator was connected to the rectifier which enabled the three-phase output to be converted into direct current. After being connected to the rectifier, the rectifier was then connected to the DC electronic load unit in which the resistive load used to test the ironless coreless electricity generator was controlled. The output voltage, as well as the output power from the ironless coreless electricity generator, were able to be monitored by using this DC electronic load unit. Other than that, the oscilloscope was used to measure the input current for the motor. Various rotational speed constant resistive load tests were carried out to examine the capability of the fabricated ironless coreless electricity generator.

In the closed circuit test on the ironless coreless generator, the same motor was used in the open circuit test. The DC electronic load was used to supply load to the ironless coreless electricity generator. In the closed circuit test, the rectifier was used to convert the alternating current generated by the ironless coreless electricity generator into the direct current. This was because the DC electronic load unit was only able to connect

by using direct current connection. Figure 3.14 shows the display of the DC electronic load used to test the ironless coreless electricity generator in the closed circuit experiment. Figure 3.15 shows the rectifier used in the closed circuit test.



Figure 3.14 DC electronic load used in the close circuit test

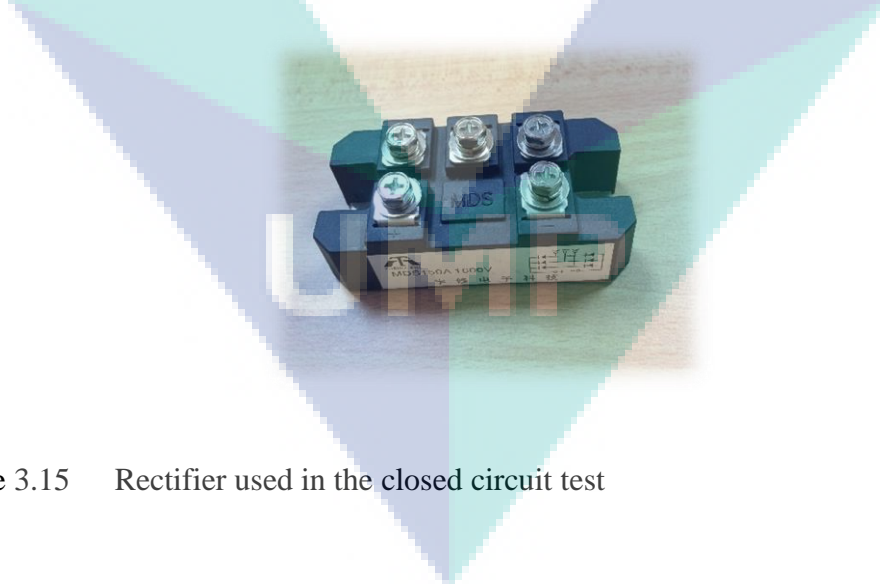


Figure 3.15 Rectifier used in the closed circuit test

The oscilloscope was used to verify the waveform profiles and the voltage was generated by the ironless coreless electricity generator passing through the rectifier. When the experiment began, the tachometer was used to measure the rotational speed of the rotors of the ironless coreless electricity generator.

When the setup was completed, the closed circuit test was performed on the ironless coreless electricity generator. After the power source was switched on, the frequency input was set on the inverter and the inverter was turned on. The motor and the rotors of the ironless coreless electricity generator started to spin. The load value was then set at the DC electronic load unit. For the various rotational speed constant load tests, the load value was set to 100 ohms. After that, the rotational speed settings of the rotors were measured using the tachometer and recorded accordingly. Screenshots of the waveform of the output voltage were also taken using the oscilloscope and transferred into the computer for further analysis. The reading of the voltage produced by the ironless coreless electricity generator, the current produced by the ironless coreless electricity generator as well as the power produced by the ironless coreless electricity generator from the DC electronic load unit were also recorded for data processing. The power input for the inverter was also measured using the current probe and voltage probe and the results were obtained by reading the output from the oscilloscope. The procedures were repeated by using various frequency inputs in the inverter as they altered the rotational speed settings of the rotors of the ironless coreless electricity generator.

The logo for UIMP (University of Malaya Power) is a large, stylized letter 'V' shape. The left side of the 'V' is light blue, the right side is a darker blue, and the bottom point is a teal color. The letters 'UIMP' are written in white, bold, sans-serif font across the center of the 'V' shape.

UIMP

CHAPTER 4

RESULTS AND DISCUSSION

4.1 Fabrication and Assembly Issue

There are a few problems during fabrication and assembly. Every issue describe in detail at every section.

4.1.1 Part Warping

The part is warped due to the material itself. Compare to iron material more toughness and not easily warping like this type of plastic material. It's more obvious on the stator (see Figure 4.1) because the thickness on stator only 12mm. The future researcher should sourcing another types of plastic which more toughness and not easily warping.

UMP



Figure 4.1 Part warping and Collision on stator of Ironless Coreless Generator

4.1.2 Collision

The collision on stator (see Figure 4.1) due to two condition. The first condition the depth of cut during machining is 1.0 mm. During the depth of cut 1.0 mm obviously can see the chip of material not cut itself (continuous chip) due to soft material. After that the depth of cut reduce to 0.5 mm to ensure the chip cut itself.

The second condition the feedrate is set 1000mm/min and contribute most factor of collision. After that the feedrate reduce to 400 mm/min. The facemill cutter diameter 50 mm used to face the surface of stator.

The factors of depth of cut, feedrate and diameter of cutter should consider well to ensure no collision happen but at the same time optimization of the cycle time.

4.1.3 Assembly coil on stator

Total 12 coils consist on stator and assembly manually one by one for every coil. The coil fixed on stator only using the tape and sponge. After assembly coil on stator done, look like the certain area thicker and can caused the rotor rubbing during spinning. It's suggested to redesign the stator, instead of only using the tape and sponge. Figure 4.2 shown, all 12 pieces of Coil assembly to Stator



Figure 4.2 The all 12 pieces of Coil assembly to Stator

4.1.4 Rubbing and Wobbling

The wobbling issue found after generator completely assembly. When tried to manually spin the shaft, the rotor obviously wobbling and rubbing the stator (see Figure 4.3). Then the generator dismantle and add the washer as improvement to solve the rubbing issue but the wobbling issue still not solved. After washer added (the total thickness of washer is around 6mm), generator then assembled again and manually spin and resulted the rotor no more rubbing on stator.

However, the increasing of air gap (previously the air gap is 20mm and after added washer the air gap become 26mm) will affect the efficiency of the ironless coreless generator.

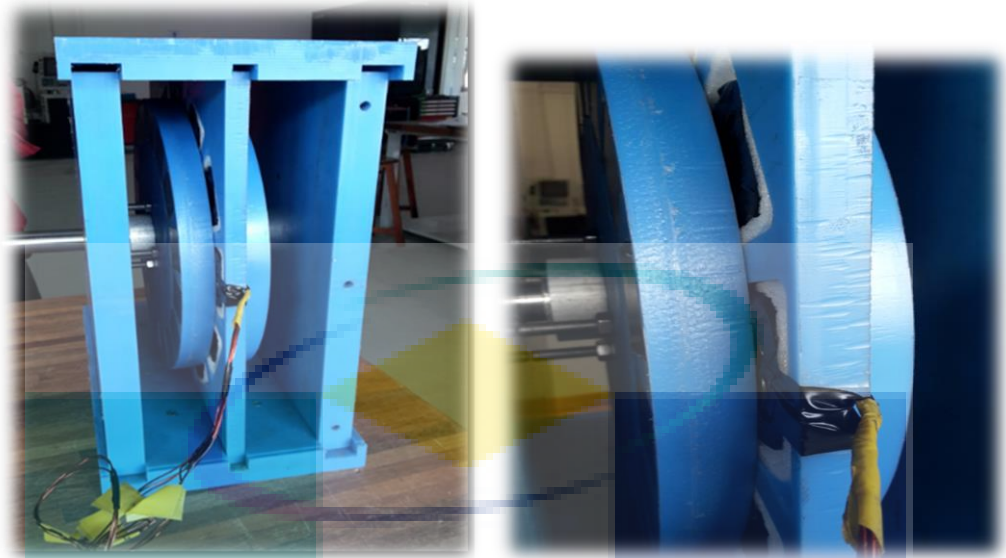


Figure 4.3 Wobbling and Rubbing when rotating the shaft

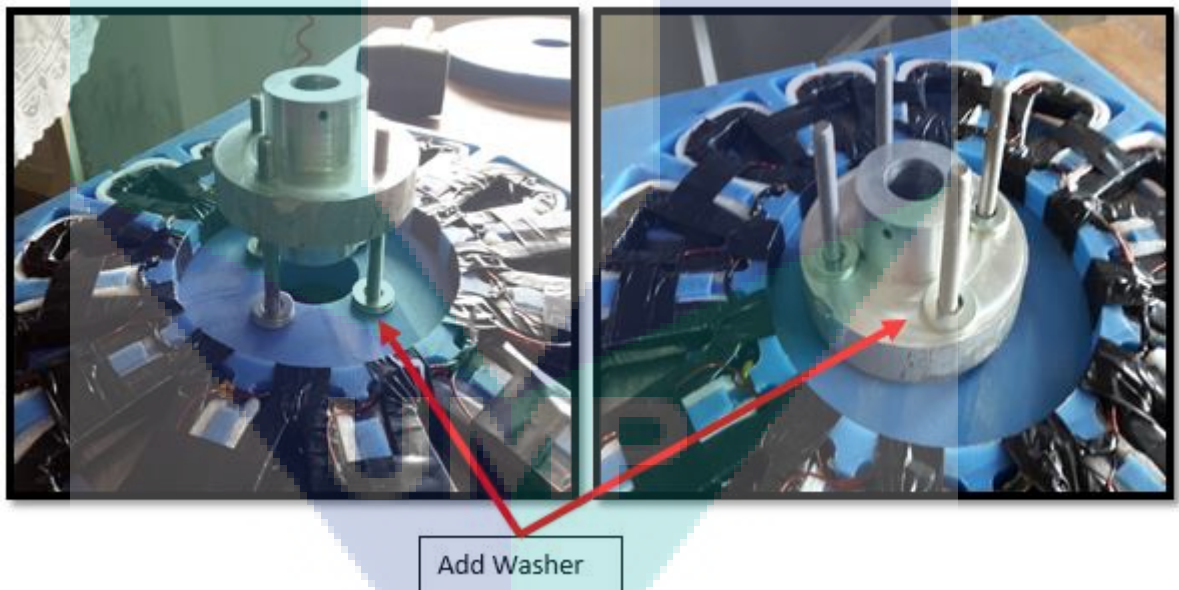


Figure 4.4 The washer was added to solve the rubbing issue.

Since the wobbling issue still not solved, it's suggested to fabricate the special jig to check the balancing of the rotor. The same concept like car tire balancing maybe can be apply to fabricate the jig (see Figure 4.5). It more obvious after assemble the magnet to the rotor, the dimension of magnet of contribute the alignment of the rotor.

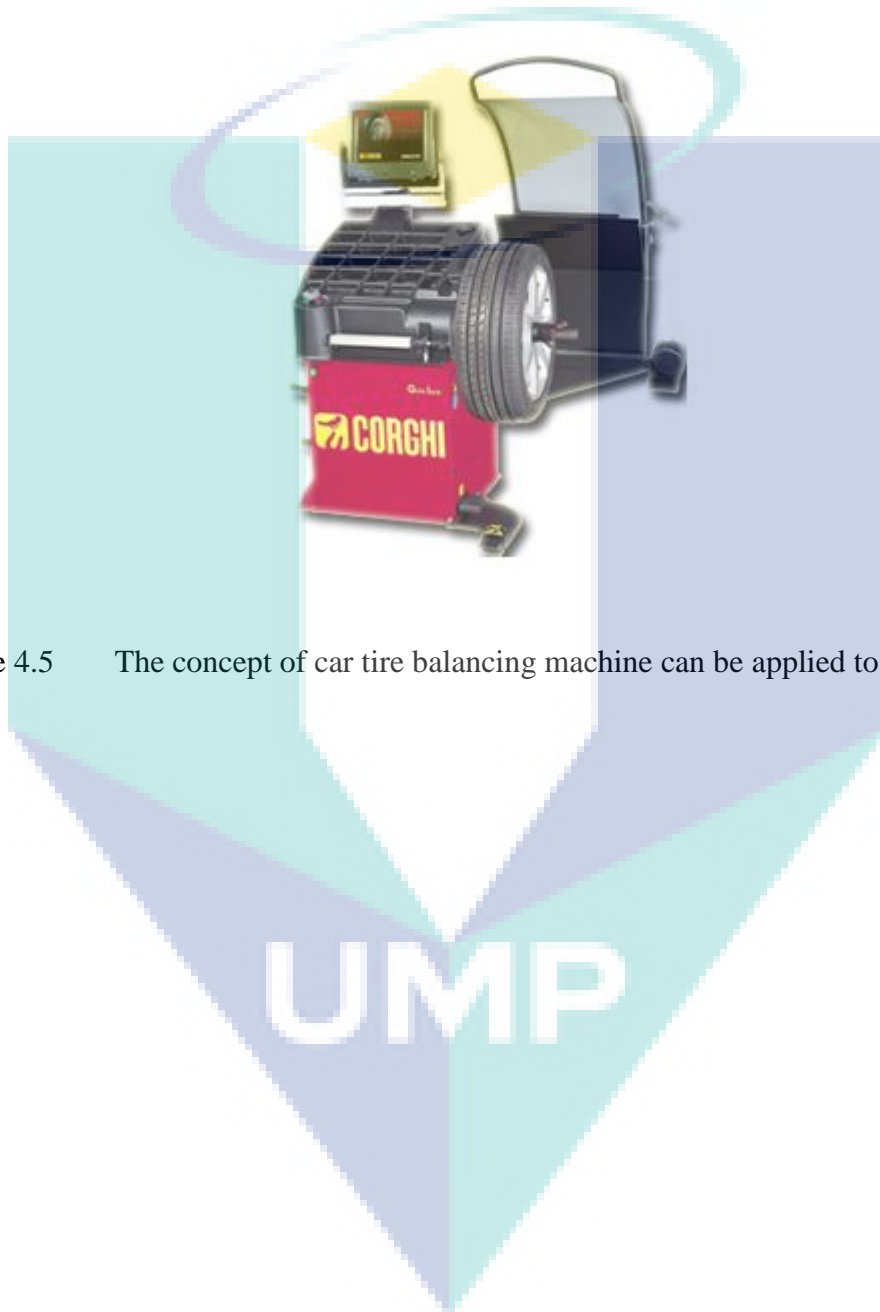


Figure 4.5 The concept of car tire balancing machine can be applied to fabricate the jig

4.2 RESULTS AND DISCUSSION OF OPEN CIRCUIT TEST

In the open circuit test, there were fifteen experiments carried out with various rotational speed settings. Figure 4.6 show the results of experiment screenshots from the oscilloscope while. Figure xx show three colors, namely, yellow, turquoise and purple, to indicate different waveforms in the graph. Each color represented the output for U-phase voltage output, V-phase voltage output and W-phase voltage output, respectively. The x-axis represented times while the y-axis represented output voltage.

The results showed the three-phase voltage output for all five experiments in the open circuit test was pure sinusoidal wave. Normally, the experimental results for other generators would not show such outcome without having done the augmentation on the output of the electricity generator. This was the selling point of this ironless coreless electricity generator because without adding extra equipment to produce or modify the output became pure sinusoidal wave, the losses in the system would be minimal. The statement regarding to the losses was supported by the findings of Tamura's research on calculation method of losses and efficiency of wind generators (Tamura, 2012)

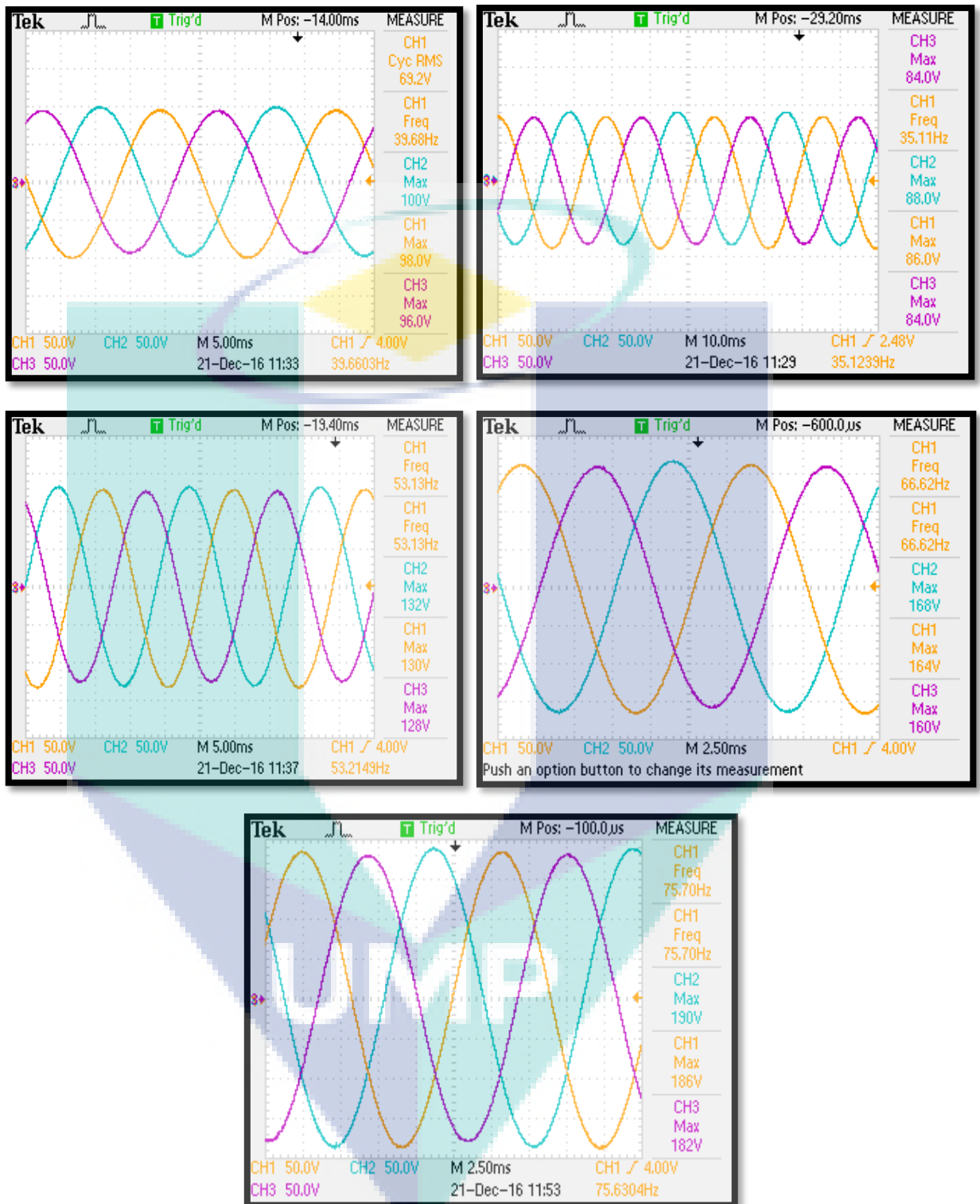


Figure 4.6 Results from oscilloscope from various rotational speed

NO LOAD TEST	ROTATIONAL SPEED (RPM)	WAVE FREQUENCY (Hz)	OUTPUT VOLTAGE (V_{rms})
1	166	22.81	39.4
2	195	27.11	47.2
3	262	35.16	61.3
4	294	39.62	69.1
5	398	53.19	92.7
6	427	58.21	101
7	465	62.81	109
8	493	66.62	116
9	528	69.64	121
10	560	75.64	131
11	690	92.42	159
12	740	100.9	163
13	1500	210.1	356
14	1671	228.8	403
15	1762	238.7	416

Table 4.1 Result output voltage and wave frequency with various rotational speed

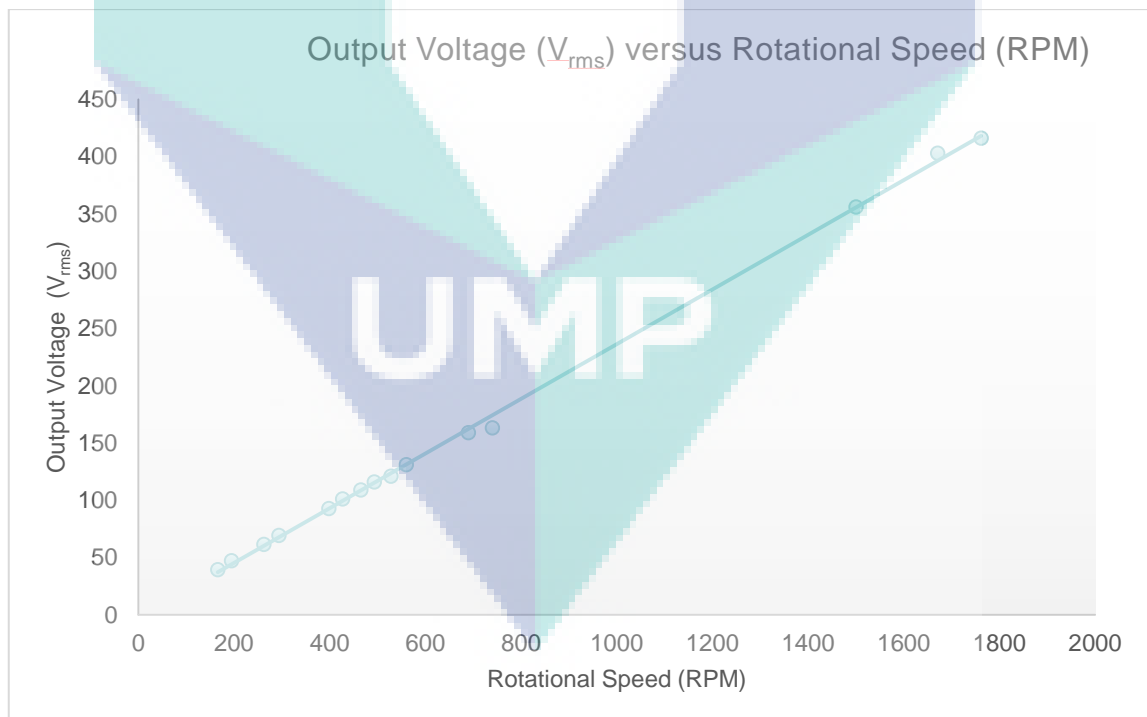


Figure 4.7 Output Voltage (V_{rms}) versus Rotational Speed (RPM) for Ironless Coreless Generator

Table 4.1 summarizes the results of open circuit test from experiment 1 to experiment 15 as illustrated in Figure xx. In experiment 1, the rotational speed used was 116RPM. It produced wave frequency of 22.81Hz with RMS value of output voltage of 39.4V. In experiment 2, the rotational speed used was 195RPM. It produced wave frequency of 27.11Hz with RMS value of output voltage of 47.2V. In experiment 3, the rotational speed used was 262RPM. It produced wave frequency of 35.16Hz with RMS value of output voltage of 61.3V. In experiment 4, the rotational speed used was 294RPM. It produced wave frequency of 39.62Hz with RMS value of output voltage of 69.1V. In experiment 5, the rotational speed used was 398RPM. It produced wave frequency of 53.19Hz with RMS value of output voltage of 92.7V.

In experiment 6, the rotational speed used was 427RPM. It produced wave frequency of 58.21Hz with RMS value of output voltage of 101V. In experiment 7, the rotational speed used was 465RPM. It produced wave frequency of 62.81Hz with RMS value of output voltage of 109V. In experiment 8, the rotational speed used was 493RPM. It produced wave frequency of 66.62Hz with RMS value of output voltage of 116V. In experiment 9, the rotational speed used was 528RPM. It produced wave frequency of 69.64Hz with RMS value of output voltage of 121V. In experiment 10, the rotational speed used was 560RPM. It produced wave frequency of 75.64Hz with RMS value of output voltage of 131V.

In experiment 11, the rotational speed used was 690RPM. It produced wave frequency of 92.42Hz with RMS value of output voltage of 159V. In experiment 12, the rotational speed used was 740RPM. It produced wave frequency of 100.9Hz with RMS value of output voltage of 163V. In experiment 13, the rotational speed used was 1500RPM. It produced wave frequency of 210.1Hz with RMS value of output voltage of 356V. In experiment 14, the rotational speed used was 1671RPM. It produced wave frequency of 228.8Hz with RMS value of output voltage of 408V. In experiment 15, the rotational speed used was 1762RPM. It produced wave frequency of 238.7Hz with RMS value of output voltage of 416V.

As shown in the illustrations Figure 4.7, it was noted that the frequency of wave became increasingly frequent and the output voltage produced by the three-phase circuit of the ironless coreless electricity generator increased within the time frame when the rotational speed of the rotors of the ironless coreless electricity generator increased. This is because when the rotors of the generator were spinning faster, the frequency of magnetic flux cutting in the three-phase circuit on the stator of the ironless coreless electricity generator increased proportionally. When there was more magnetic flux cut by the three-phase circuit in the stator, the voltage per phase and wave frequency of each phase produced by the ironless coreless electricity generator also increased. This explanation for the open circuit test is similar and agrees with that of Chalmers and Spooner's research findings on an axial flux permanent magnet generator for a gearless wind energy system (Chalmers & Spooner, 1999).

4.2.1 Verification No of Pole

The ironless coreless generator consist 16 poles on rotor. From equation 2.7 rotational speed can be verified using wave frequency from oscilloscope. Referring to example 1, No load test 1, wave frequency from oscilloscope was 22.81Hz, filled in into equation 2.7, rotational speed from formula was 171RPM, the actual rotational speed from tachometer was 166RPM, and the deviation was 2.9%. From example 2, No load test 5, wave frequency from oscilloscope was 53.19Hz, filled in into equation 2.7, rotational speed from formula was 399RPM, the actual rotational speed from tachometer was 398RPM, and the deviation was 0.25%. From example 3, No load test 10, wave frequency from oscilloscope was 75.64Hz, filled in into equation 2.7, rotational speed from formula was 567RPM, the actual rotational speed from tachometer was 560RPM, and the deviation was 1.2%. From example 4, No load test 15, wave frequency from oscilloscope was 238.7Hz, filled in into equation 2.7, rotational speed from formula was 1790RPM, the actual rotational speed from tachometer was 1762RPM, and the deviation was 1.7%.

Mostly the deviation data less than 3%, it was because the wave frequency value from oscilloscope was fluctuate. By applying the rotational speed of the rotors of the

generator and the frequency output produced by the rotors as indicated in Eq. 2.7, the calculated result was in good agreement with the ironless coreless electricity generator design, that is, 16 poles applied on a rotor.

$$N = \frac{120f}{p} \quad (2.7)$$

Where;

N represents rotational speeds of the rotors in RPM,

f represents frequency of the rotors and

p represents number of poles on each rotor

Example 1;

Test Load 1, $f = 22.81$

$N = 120 (22.81) / 16 = 171 \text{ RPM}$

Actual RPM = 166 RPM

Deviation = $((171 - 166) / 171) \times 100 = 2.9\%$

Example 2;

Test Load 5, $f = 53.19$

$N = 120 (53.19) / 16 = 399 \text{ RPM}$

Actual RPM = 398 RPM

Deviation = $((399 - 398) / 399) \times 100 = 0.25\%$

Example 3;

Test Load 10, $f = 75.64$

$N = 120 (74.64) / 16 = 567 \text{ RPM}$

Actual RPM = 560 RPM

Deviation = $((567 - 560) / 567) \times 100 = 1.2\%$

Example 4;

Test Load 15, $f = 238.7$

$N = 120 (238.7) / 16 = 1790 \text{ RPM}$

Actual RPM = 1762 RPM

Deviation = $((1790 - 1762) / 1790) \times 100 = 1.7\%$

4.2.2 Different Amplitude Each Phase Voltage

From observation on oscilloscope found (refer Figure 4.8), the amplitude each phase little bit different. Base on theory, the amplitude each phase supposedly same. Then the data with rotational speed recorded and fill in the Table 4.2. From test no 1 until test no 12, the lowest differentiation value was 2 volts and the maximum differentiation was 10 volts. Increasing differentiation value is proportional with rotational speed. Highlighted with different colors, brown, blue and purples, each colors represent phase 1, phase 2 and phase 3 respectively. The phase 3 shows the lowest value, follow by phase 1 and the highest value is phase 2.

The coil produce the output voltage in these ironless coreless generator. The highest possibility the amplitude every phase not same due to no of turns of coils in stator. The coiling process perform manually using special jig (refer Figure 4.9). Every coils consist 125 turns and every phase consist 500 turns. Human mistake due to count wrongly cause the output voltage produce not same. To tackle this problem, the improvement on the jig is must like make a fully automatic to count the no of turns.

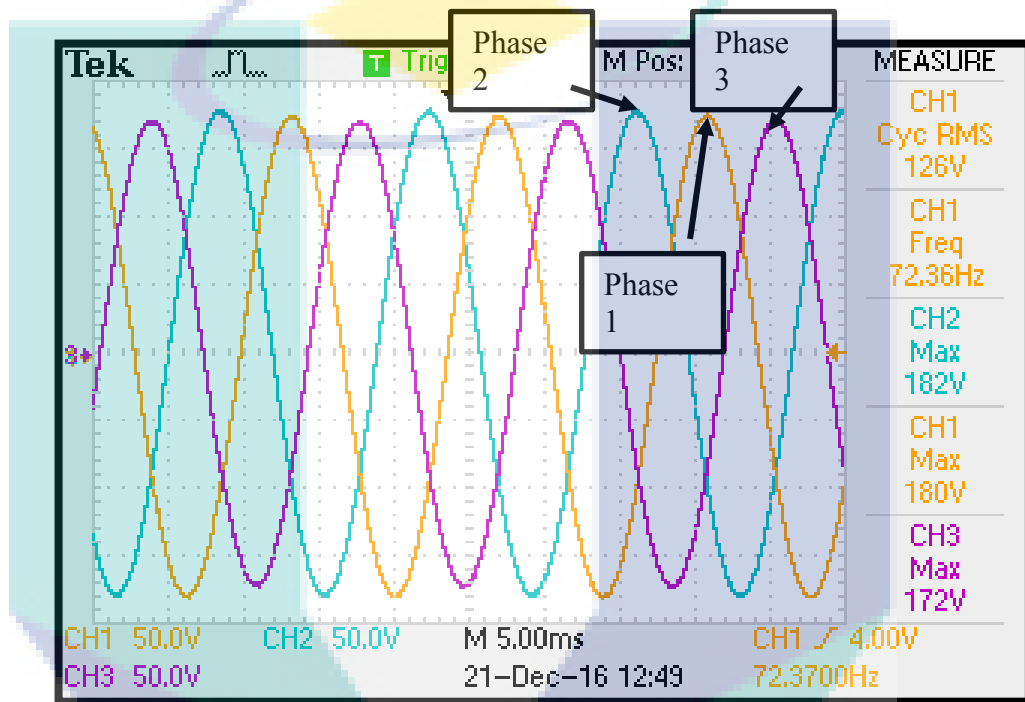


Figure 4.8 The different amplitude each phase

NO LOAD TEST	ROTATIONAL SPEED (RPM)	V_{max}			Different (max- min)			
		Phase 1	Phase 2	Phase 3				
1	166	56	58	56	2			
2	195	68	68	66	2		Low	
3	262	88	90	84	6		Medium	
4	294	98	100	96	4		High	
5	398	132	134	128	6			
6	427	144	146	140	6			
7	465	156	158	150	8			
8	493	164	168	160	8			
9	528	172	174	168	6			
10	560	188	190	182	8			
11	690	228	230	220	10			
12	740	236	238	230	8			

Table 4.2 The data of different amplitude each phase

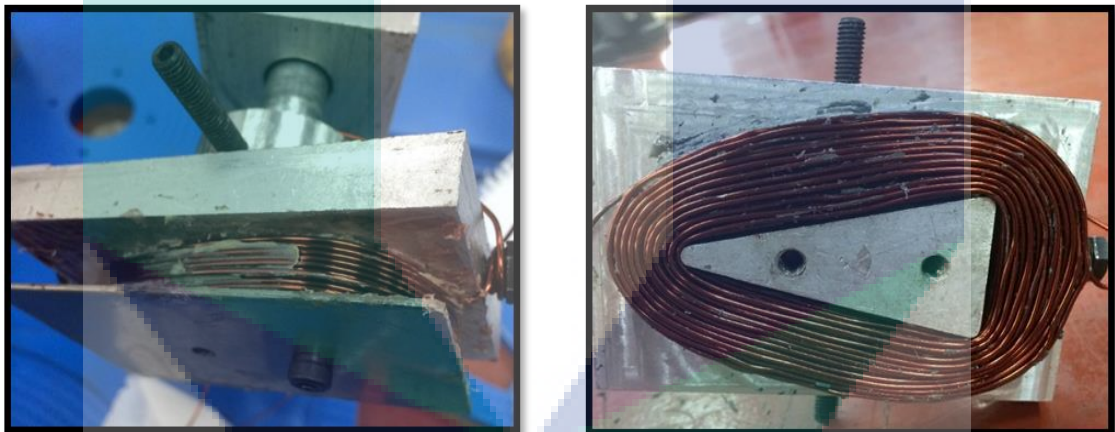


Figure 4.9 Coiling process perform manually using special jig

4.2.3 The Waveform Not Sinusoidal At Certain Speed

During the experiment, at rotational speed exceed 700 rpm the waveform every phase become not sinusoidal anymore. The shape of waveform become worst proportional increasing the rotational speed. The first assumption the waveform become not sinusoidal due to voltage retention. After double check the probe used (see Figure 4.11) only can reach maximum voltage 300 volts only. Then probe replaced with higher voltage probe which can reach maximum value 1000 volts. Luckily after probe replacement, the waveform become sinusoidal back. Even at maximum rotational speed ~1800rpm the waveform still maintain pure sinusoidal.

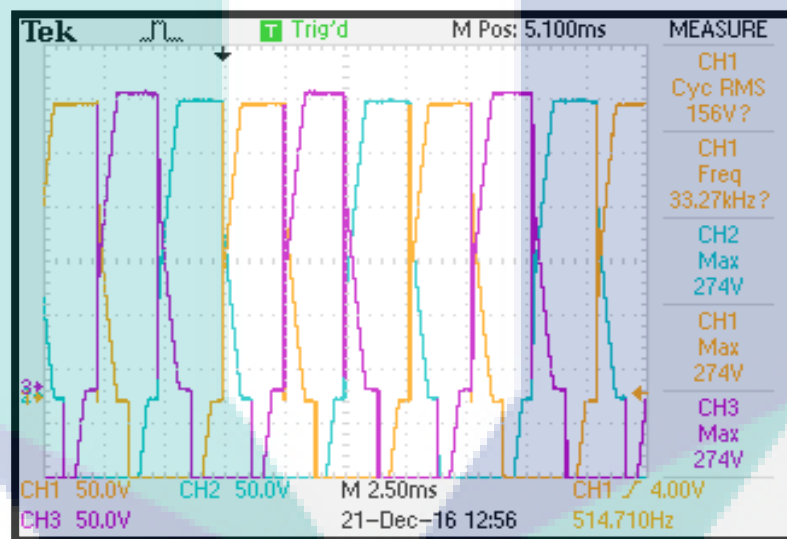


Figure 4.10 Waveform not sinusoidal at certain rotational speed

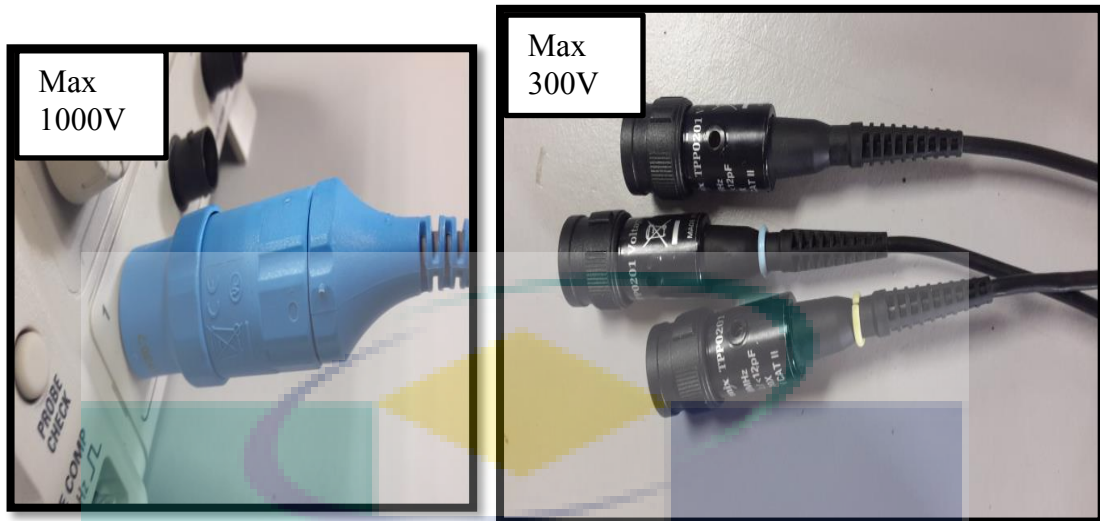


Figure 4.11 Different types of probe. The probe with blue color can reach maximum 1000V and probe with black color only can reach maximum 300V

4.3 RESULTS AND DISCUSSION OF CLOSED CIRCUIT TEST

The results of the closed circuit test on the ironless coreless electricity generator will be presented and discussed. After the open circuit test was done, the closed circuit test or loaded test was performed to test the ironless coreless electricity generator. The reason to perform the closed circuit test was to experiment the capabilities of the fabricated ironless coreless electricity generator under loaded conditions.

In the various rotational speed constant load tests, the load used by the ironless coreless electricity generator was set as constant variable, which was 100 ohm (see Table 4.3). There were 9 sets of experiments carried out in the various rotational speed constant load tests. In the first run, rotational speed of 104RPM was used on the rotor of the ironless coreless electricity generator. With such rotational speed, the ironless coreless electricity generator was able to produce output power of 9.33W, current 0.3A and output voltage of 30.54V. Rotational speed of 137RPM was used on the rotors of the generator during the second test. The generator was able to produce output power of 16.27W, current 0.4A and output voltage of 40.34V.

In the third experiment, rotational speed of 212RPM was set on the rotor of the ironless coreless electricity generator. The generator was able to produce output power of 39.3W, current 0.6A and output voltage of 62.69V. The fourth experiment, rotational speed of 240RPM was set on the rotor of the ironless coreless electricity generator. The generator was able to produce output power of 49.53W, current 0.7A and output voltage of 70.38V. The fifth experiment, rotational speed of 298RPM was set on the rotor of the ironless coreless electricity generator. The generator was able to produce output power of 76.97W, current 0.9A and output voltage of 87.73V.

The sixth experiment, rotational speed of 350RPM was set on the rotor of the ironless coreless electricity generator. The generator was able to produce output power of 107.66W, current 1.0A and output voltage of 103.76V. The seventh experiment, rotational speed of 423RPM was set on the rotor of the ironless coreless electricity generator. The generator was able to produce output power of 144.99W, current 1.2A and output voltage of 120.41V. The eighth experiment, rotational speed of 455RPM was set on the rotor of the ironless coreless electricity generator. The generator was able to produce output power of 182.12W, current 1.3A and output voltage of 134.95V. The ninth experiment, rotational speed of 523RPM was set on the rotor of the ironless coreless electricity generator. The generator was able to produce output power of 236.64W, current 1.5A and output voltage of 153.18V.



UMP

LOAD TEST	LOAD (Ohm)	ROTATIONAL SPEED (RPM)	POWER (Watt)	VOLTAGE (V)	CURRENT (A)
1	100	104	9.33	30.54	0.3
2	100	137	16.27	40.34	0.4
3	100	212	39.3	62.69	0.6
4	100	240	49.53	70.38	0.7
5	100	298	76.97	87.73	0.9
6	100	350	107.66	103.76	1.0
7	100	423	144.99	120.41	1.2
8	100	455	182.12	134.95	1.3
9	100	523	236.64	153.18	1.5

Table 4.3 Results for power output in various rotational speed constant load tests

In the various rotational speed constant load tests carried out on the ironless coreless electricity generator, when the rotational speed of the rotors of the generator increased, the power generated by the ironless coreless electricity generator also increased. Likewise, for the ironless coreless electricity generator, when the rotational speed of the rotor in the ironless coreless electricity generator increased, the magnetic flux cutting rate for the coil connected using three-phase star connection on the stator also increased. When such phenomena occurred, more voltage and current would be produced by the three-phase coil on the stator of the ironless coreless electricity generator. Assuming that the load used by the ironless coreless electricity generator was constant, when the current produced by the ironless coreless electricity generator increased, the power generated by the ironless coreless electricity generator also increased. The results for the various rotational speed constant load tests for the ironless coreless electricity generator in this research showed similar trend with the results in Chung and Yew's research for their coreless axial-flux permanent-magnet generator for small wind turbines (Chung & You, 2014).

Figure 4.12 shows the graph for the power generated by ironless coreless electricity generator versus rotational speed of the rotors of the generator. The output power generated by the generator from around 9W increased to around 236W when the rotational speed of the rotors of the generator rose from 104RPM to 523RPM.

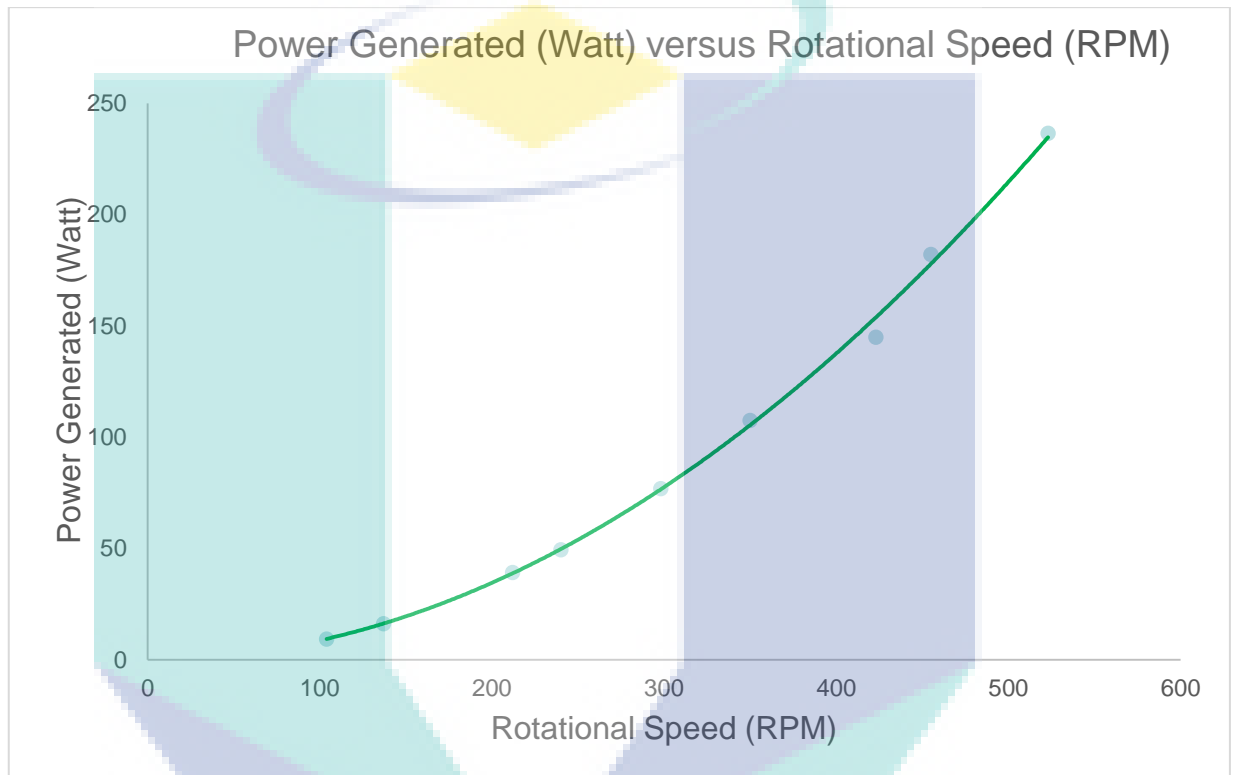


Figure 4.12 Power generated by ironless coreless electricity generator versus rotational speed graph

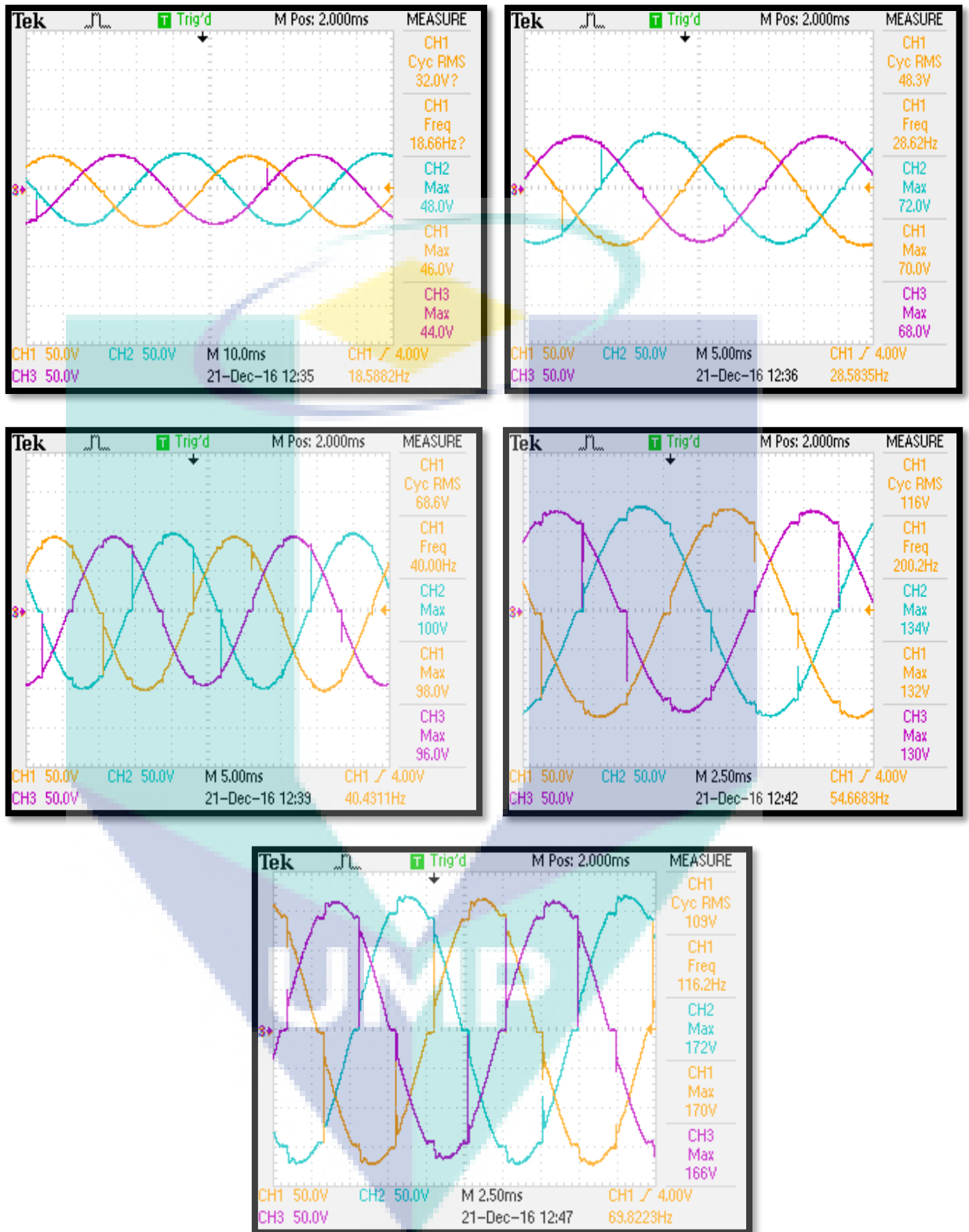


Figure 4.13 Waveform characteristic on closed circuit test.

In the closed circuit test on the fabricated ironless coreless electricity generator, there was a ripple within the waveform obtained from the oscilloscope (refer Figure 4.13). The waveform obtained during the test was not so smooth compared to the waveform obtained during the open circuit test. It is believed that there was some noise or interference which had occurred within the system itself when the system was connected to the rectifier. This was because when the circuits was connected to the silicon-controlled rectifiers, “notching” effects occurred, and when these devices were doing switching operation, it caused sharp inverted spikes during commutation or transfer of conduction from one phase to the next (Vijayaraghavan, Brown & Barnes, 2008). To reduce the ripple, should apply the filter like inductor and capacitor after the rectifier, so that the filtered output voltage of the ironless coreless electricity generator will be smoother (Liang, Yang & Chen, 2007; Nishimura et al., 2008).



UMP

CHAPTER 5

CONCLUSION AND SUGGESTION

5.1 Conclusion

At the end of the research both objectives achieved, the ironless coreless electricity generator was successfully fabricated and tested with maximum rotational speed $\sim 1800\text{RPM}$ and producing output voltage $\sim 416\text{Vrms}$. The part replacement involved one piece of stator and two pieces of the rotor using CNC Milling Machine. All the issued during fabrication and assembly process has been tackled perfectly.

The ironless coreless generator involved two testing, open circuit testing (also known no load testing) and closed circuit testing (also known load testing). Each phase of a waveform shown pure sinusoidal wave in open circuit test. The output voltage proportional with rotational speed. The pure achievement when the generator can spin with full rotational speed $\sim 1800\text{ RPM}$ and generated output voltage $\sim 416\text{Vrms}$. During the closed circuit test, the ripple appears on sinusoidal wave and the increasing of ripple proportional with rotational speed. The ripple caused by some noise or interference.

5.2 Suggestions

There are a few suggestions which can be done to improve the current version of ironless coreless electricity generator in this research. First of all, to further improve the efficiency of the ironless coreless electricity generator, it is suggested to fabricate the special jig to ensure the rotor can spin without wobbling after assembly the magnet. The same concept maybe can be applied like car tyre balancing machine. It is important to ensure after all components assembled the rotor not rubbing the stator while spinning.

In addition, to further reduce the wobbling and rubbing issue, another alternative ironless material or another types of plastic material should be source. The current material easily tend to warping during machining.

Finally, it would be an interesting research if an increase in the number of rotors and stators of the ironless coreless electricity generator can be made without changing its original design as this might be the way to further increase the output power of the ironless coreless electricity generator.



UMP

REFERENCES

- Ahmed D. and Ahmad A. (2013). *An optimal design of coreless direct-drive axial flux permanent magnet generator for wind turbine*. **Journal of Physics: Conference Series** **439** (2013) 012039
- Ahmed D. and Ahmad A. (2013). *An optimal design of coreless direct-drive axial flux permanent magnet generator for wind turbine*. **Journal of Physics: Conference Series** **439** (2013) 012039
- Breton, C., Bartolome, J., Benito, J. A., Tassinario, G., Flotats, I., Lu, C. W. and Chalmers, B. J. (2000). Influence of machine symmetry on reduction of cogging torque in permanent-magnet brushless motors. *Magnetics, IEEE Transactions on*, **36**(5), 3819-3823.
- Bumby, J. R. and Martin, R. (2005). Axial-flux permanent-magnet air-cored generator for small-scale wind turbines. *IEE Proceedings-Electric Power Applications*, **152**(5), 1065-1075.
- Chalmers, B. J. and Spooner, E. (1999). An axial-flux permanent-magnet generator for a gearless wind energy system. *Energy Conversion, IEEE Transactions on*, **14**(2), 251-257.
- Chan, T. F. and Lai, L. L. (2007). *An axial-flux permanent-magnet synchronous generator for a direct-coupled wind-turbine system*. **Energy Conversion, IEEE Transactions on**, **22**(1), 86-94.
- Chung, D. W. and You, Y. M. (2014). Design and Performance Analysis of Coreless Axial-Flux Permanent-Magnet Generator for Small Wind Turbines. *Journal of Magnetics*, **19**(3), 273-281.
- Del Ferraro, L., Giulii Capponi, F., Terrigi, R., Caricchi, F. and Honorati, O. (2006, October). Ironless axial flux PM machine with active mechanical flux weakening for automotive applications. *Industry Applications Conference, 2006. 41st IAS Annual Meeting. Conference Record of the 2006 IEEE* (Vol. 1, pp. 1-7). IEEE.
- Drazikowski, L. and Koczara, W. (2011). Permanent magnet disk generator with coreless windings. *COMPEL: The International Journal for Computation and Mathematics in Electrical and Electronic Engineering*, **31**(1), 108-118.
- Gieras, J. F., Wang, R. J. and Kamper, M. J. (2008). *Axial flux permanent magnet brushless machines (Vol. 1)*. New York, NY: Springer.
- Gor, H. and Kurt, E. (2016). Waveform characteristics and losses of a new double sided axial and radial flux generator. *International Journal of Hydrogen Energy*.

Hosseini, S. M., Agha-Mirsalim, M. and Mirzaei, M. (2008). *Design, Prototyping, and Analysis of a Low Cost Axial-Flux Coreless Permanent-Magnet Generator*. **IEEE Transaction on Magnetics**, Vol. 44, No. 1, January 2008

Huang, S., Luo, J., Leonardi, F. and Lipo, T. A. (1999). A comparison of power density for axial flux machines based on general purpose sizing equations. *Energy Conversion, IEEE Transactions on*, 14(2), 185-192.

Hwang, C. C., Li, P. L., Chuang, F. C., Liu, C. T. and Huang, K. H. (2009). Optimization for reduction of torque ripple in an axial flux permanent magnet machine. *Magnetics, IEEE Transactions on*, 45(3), 1760-1763.

Javadi, S. and Mirsalim, M. (2010). Design and analysis of 42-V coreless axial-flux permanent-magnet generators for automotive applications. *Magnetics, IEEE Transactions on*, 46(4), 1015-1023.

Kobayashi, H., Doi, Y., Miyata, K. and Minowa, T. *Design of axial-flux permanent magnet coreless generator for the multi-megawatts wind turbines*. **EWEC2009**.

Kurt, E., Gör, H. and Demirtaş, M. (2014). Theoretical and experimental analyses of a single phase permanent magnet generator (PMG) with multiple cores having axial and radial directed fluxes. *Energy Conversion and Management*, 77, 163-172

Li, H. and Chen, Z. (2008). *Overview of different wind generator systems and their comparisons*. **IET Renewable Power Generation**, 2(2), 123-138.

Li, S., Haskew, T. A. and Xu, L. (2010). Conventional and novel control designs for direct driven PMSG wind turbines. *Electric Power Systems Research*, 80(3), 328-338.

Lombard, N. F. and Kamper, M. J. (1999). Analysis and performance of an ironless stator axial flux PM machine. *Energy Conversion, IEEE Transactions on*, 14(4), 1051-1056.

Madawala, U. K. and Boys, J. T. (2005). Magnetic field analysis of an ironless brushless dc machine. *Magnetics, IEEE Transactions on*, 41(8), 2384-2390.

Mahmoudi, A., Kahourzade, S., Rahim, N. A., Ping, H. W. and Uddin, M. N. (2013). Design and prototyping of an optimised axial-flux permanent-magnet synchronous machine. *Electric Power Applications, IET*, 7(5), 338-349.

Mahmoudi, A., Rahim, N. A. and Hew, W. P. (2011). Axial-flux permanent-magnet machine modeling, design, simulation, and analysis. *Scientific Research and Essays*, 6(12), 2525-2549.

Mirzaei, M., Mirsalim, M. and Abdollahi, S. E. (2007). Analytical modeling of axial air gap solid rotor induction machines using a quasi-three-dimensional method. *Magnetics, IEEE Transactions on*, **43**(7), 3237-3242.

Mo, W., Zhang, L., Shan, A., Cao, L., Wu, J. and Komuro, M. (2008). Improvement of magnetic properties and corrosion resistance of NdFeB magnets by intergranular addition of MgO. *Journal of Alloys and Compounds* **461**(1), 351-354.

Molina, M. G., dos Santos, E. C. and Pacas, M. (2010, September). Advanced power conditioning system for grid integration of direct-driven PMSG wind turbines. *Energy Conversion Congress and Exposition (ECCE), 2010 IEEE* (pp. 3366-3373). IEEE.

Muljadi, E., Butterfield, C. P. and Wan, Y. H. (1999). Axial-flux modular permanent-magnet generator with a toroidal winding for wind-turbine applications. *Industry Applications, IEEE Transactions on*, **35**(4), 831-836.

Nishimura, K., Hirachi, K., Komiyama, S. and Nakaoka, M. (2008, February). Two buck choppers built-in single phase one stage pfc converter with reduced DC voltage ripple and its specific control scheme. *Applied Power Electronics Conference and Exposition, 2008. APEC 2008. Twenty-Third Annual IEEE* (pp. 1378-1383). IEEE.

Oh, S. C. and Emadi, A. (2004). Test and simulation of axial flux-motor characteristics for hybrid electric vehicles. *Vehicular Technology, IEEE Transactions on*, **53**(3), 912-919.

Parviainen, A., Niemelä, M. and Pyrhönen, J. (2004). Modeling of axial flux permanent-magnet machines. *Industry Applications, IEEE Transactions on*, **40**(5), 1333-1340.

Pop, A. A., Jurca, F., Oprea, C., Chirca, M., Breban, S. and Radulescu, M. M. (2013, September). Axial-flux vs. radial-flux permanent-magnet synchronous generators for micro-wind turbine application. *Power Electronics and Applications (EPE), 2013 15th European Conference on* (pp. 1-10). IEEE.

Rizzoni, G. (2007). *Principle and Applications of Electrical Engineering 5th edition*. McGraw-Hill Higher Education.

Samarins.com. Alternator, How It Works, Symptoms, Testing, Problems, Replacement. Retrieved from <http://www.samarins.com/glossary/alternator.html>

Spooner, E. and Chalmers, B. J. (1992). TORUS': a slotless, toroidal-stator, permanent-magnet generator. *Electric Power Applications, IEE Proceedings B*, **139**(6), 497-506.

Stampfi, H. (2003). Linear motor applications: Ironcore versus Ironless Solution. Retrieved from http://www.controldesign.com/assets/Media/MediaManager/wp_035_etel_thompson.pdf

Storr W. (2013). *Transformer Construction*. Electronics-Tutorials.ws. Retrieved from <http://www.electronics-tutorials.ws/transformer/transformer-construction.html>

Tamura, J. (2012). Calculation method of losses and efficiency of wind generators. *Wind Energy Conversion Systems* (pp. 25-51). Springer London.

Ting, C. C. and Yeh, L. Y. (2014). Developing the full-field wind electric generator. *International Journal of Electrical Power & Energy Systems*, **55**, 420-428.

Vijayaraghavan, G., Brown, M. and Barnes, M. (2008). Electrical noise and mitigation-Part 1: Noise definition, categories and measurement.

Virtic, P. and Avsec, J. (2011). Analysis of coreless stator axial flux permanent magnet synchronous generator characteristics by using equivalent circuit. *Przegląd Elektrotechniczny*, **87**(3), 208-211.

Wang, R. J., Kamper, M. J., Van der Westhuizen, K. and Gieras, J. F. (2005). Optimal design of a coreless stator axial flux permanent-magnet generator. *Magnetics, IEEE Transactions on*, **41**(1), 55-64.

Z. Zhang, A. Chen, A. Matveev, R. Nilssen, and A. Nysveen, 'High-power generators for offshore wind turbines', *Energy Procedia* **35** (2013) 52 – 61.

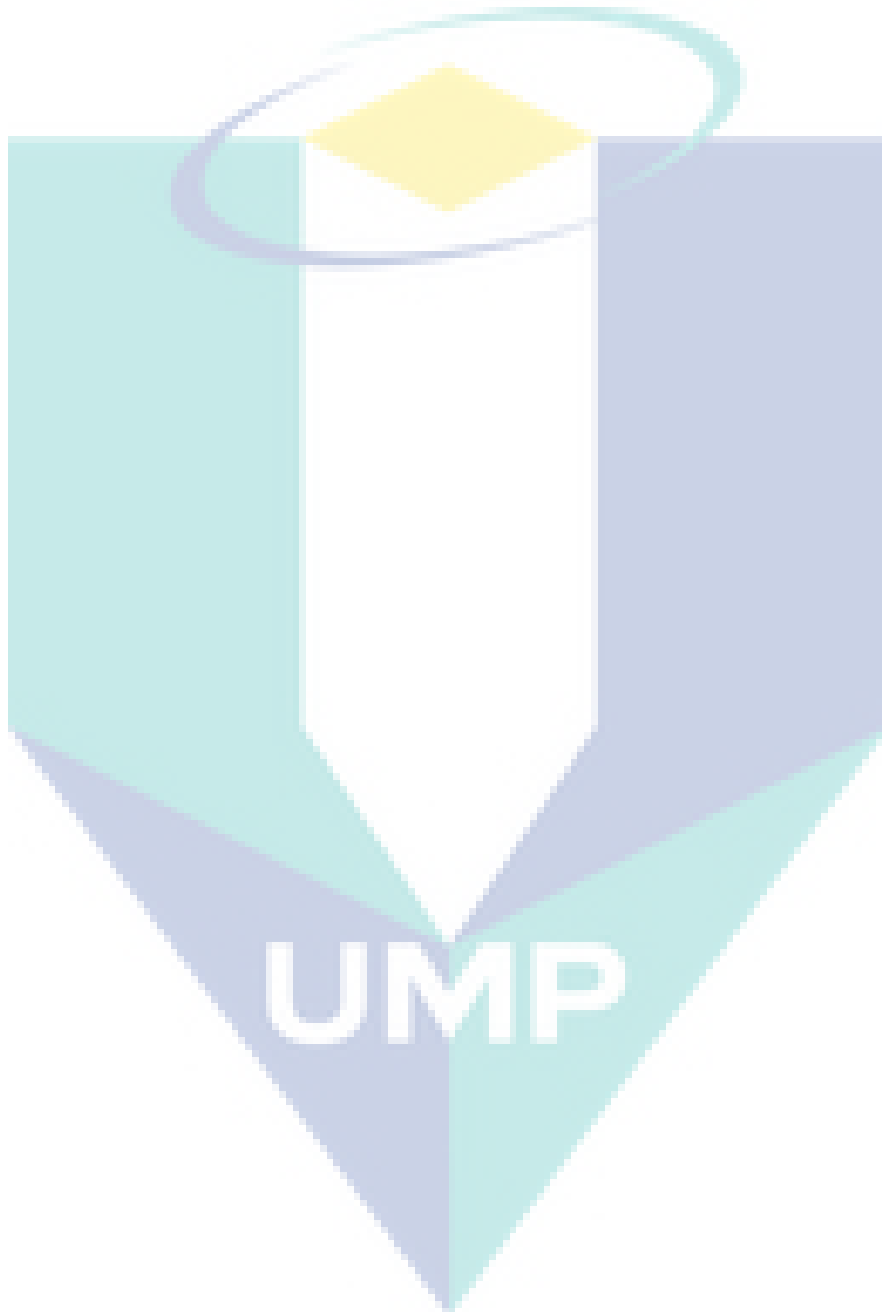
Zhang, S., Tseng, K. J., Vilathgamuwa, D. M., Nguyen, T. D. and Wang, X. Y. (2011). Design of a robust grid interface system for PMSG-based wind turbine generators. *Industrial Electronics, IEEE Transactions on*, **58**(1), 316-328.

The logo for UMP (Universiti Malaysia Perlis) is a large, stylized letter 'V' shape. The left side of the 'V' is light blue, the right side is light green, and the bottom point is a darker blue. The letters 'UMP' are written in white, bold, sans-serif font across the center of the 'V' shape.

UMP

APPENDIX A
SAMPLE APPENDIX 1

For Appendices Heading, use TITLE AT ROMAN PAGES style.



APPENDIX B
SAMPLE APPENDIX 2

For Appendices Heading, use TITLE AT ROMAN PAGES style.

